INVESTIGATING THE ROLE OF CELLULAR AUTOPHAGY IN HUMAN MONOCYTIC CELL DEATH BY KINOME ANALYSIS

A Thesis Submitted to the College of

Graduate Studies and Research

In Partial Fulfillment of the Requirements

For the Degree of Master of Science

In the Vaccinology and Immunotherapeutics Program

School of Public Health

University of Saskatchewan

Saskatoon, Saskatchewan, Canada

By

Rylan Bridge

Permission to Use

In presenting this thesis/dissertation in partial fulfillment of the requirements for a Postgraduate degree from the University of Saskatchewan, I agree that the Libraries of this University may make it freely available for inspection. I further agree that permission for copying of this thesis/dissertation in any manner, in whole or in part, for scholarly purposes may be granted by the professor or professors who supervised my thesis/dissertation work or, in their absence, by the Head of the Department or the Dean of the College in which my thesis work was done. It is understood that any copying or publication or use of this thesis/dissertation or parts thereof for financial gain shall not be allowed without my written permission. It is also understood that due recognition shall be given to me and to the University of Saskatchewan in any scholarly use which may be made of any material in my thesis/dissertation.

Requests for permission to copy or to make other uses of materials in this thesis/dissertation in whole or part should be addressed to:

Director, Vaccinology and Immunotherapeutics Program

School of Public Health

University of Saskatchewan

Saskatoon, Saskatchewan S7N 5E5

Abstract

Cells of the Monocyte / Macrophage lineage are key players in innate and adaptive immunity. They eliminate pathogens through their phagocytic and antimicrobial properties, secretion of inflammatory and immunoregulatory cytokines, as well as their capacity to present foreign antigens to T lymphocytes in lymphoid tissues. The importance of M/Ms in the immune response require them to undergo strict regulation, which occurs, at least in part, through the control of monocytic cell survival. Autophagy is a ubiquitous cellular process by which cells degrade intracellular, cytoplasmic components via a network of interconnected vacuoles to carry out a variety of functions. Autophagy typically functions in maintaining cellular homeostasis and mitigating stresses. However, more recent studies have shown that autophagy may play a role in cell death.

Our laboratory has previously found that the cytokine IFNγ can induce cell death in human monocytes in an autophagy-dependent manner. Conversely, IL-10 inhibits both spontaneous and IFNγ-induced cell death, a capacity that ironically, is also associated with the induction of autophagy. We are thus interested in understanding how the autophagy pathway can play a dual role in human monocyte survival. Interestingly, a novel autophagy-inducing antimicrobial peptide (Atg peptide) was recently shown to be capable of inducing an autophagy-dependent form of cell death. In this study, I established an *in vitro* model for Atg peptide-induced cell death in human monocytic cells. Subsequently, I designed and tested an autophagy- and cell death pathway-centric kinome microarray in order to begin elucidating the molecular mechanisms responsible for monocytic cell death. Kinome analysis identified several interesting phosphorylation events in response to Atg peptide stimulation, including the tumour suppressor protein p53, which was phosphorylated at S9, an Na+,K+-ATPase ATP1A1 which was phosphorylated at Y10, and the

transcription factor 4E-BP1 which was phosphorylated at S65. I confirmed these phosphorylation results in part using Western blotting. Finally, I present several hypotheses for the potential molecular mechanisms involved in Atg peptide-induced autophagic cell death in monocytes revealed by kinome analysis, which provide a basis for further exploration into this extremely interesting area.

Acknowledgements

I would like to thank my supervisors, Dr. Marko Kryworuchko and Dr. Suresh Tikoo, for their crucial guidance through this journey. I would additionally like to thank Dr. Philip Griebel, Dr. Scott Napper and Marylin Rana for their patience and support as part of my graduate committee, and the collaboration of Dr. Ildiko Badea. I would also extend thanks to my friends and colleagues in the lab, especially Cathy Hutchinson, Jin Ha Yang, Luke Truitt, Cherise Hedlin, Sam Ekanayake, and Nolan Rau, for their assistance and kindness. This research would not have been possible without financial support from the Canadian Institutes of Health Research and the Saskatchewan Health Research Foundation, which we gratefully acknowledge. Lastly, I would like to thank my friends and family, and especially my parents, for their never-ending support over the years.

Table of Contents

List of Tables

List of Figures

List of Abbreviations

Ab	antibody
APC	antigen-presenting cell
APS	ammonium persulphate
ATPase	adenosinetriphosphatase
Bad	Bcl-2 antagonist of cell death
BSA	bovine serum albumin
CD14	cluster of differentiation 14
CD4	cluster of differentiation 4
CD8	cluster of differentiation 8
DAMP	damage-associated molecular pattern
EDTA	ethylenediaminetetraacetic acid
EGTA	ethylene glycol-bis(β-aminoethyl ether)-N,N,N',N'-tetraacetic acid
ER	endoplasmic reticulum
FC	fold-change
GAPDH	glyceraldehyde 3-phosphate dehydrogenase
GM-CSF	granulocyte macrophage colony-stimulating factor
HEPES	4-(2-hydroxyethyl)-1-piperazineethanesulfonic acid
IFNγ	interferon gamma
IgG	immunoglobulin G
IL-10	interleukin 10
IL-18	interleukin 18
IL-1β	interleukin 1 beta
IL-4	interleukin 4
JNK	c-Jun N-terminal kinase 1
LAP	LC3-associated phagocytosis
LC3	microtubule-associated proteins 1A/1B light chain 3A
MACS	magnetic activated cell sorting
M/M	monocyte and macrophage
MAPK	mitogen-activated kinase
M-CSF	macrophage colony-stimulating factor

MHC	major histocompatibility complex
MyD88	myeloid differentiation primary response 88
NF-κB	nuclear factor-κB
NLR	nucleotide-binding oligomerization domain-like receptor
PAMP	pathogen-associated molecular pattern
PBMC	peripheral blood mononuclear cell
PBS	phosphate-buffered saline
PCD	programmed cell death
PD	Parkinson's disease
PE	phycoerythrin
PI	propidium iodide
PIIKA	Platform for Intelligent, Integrated Kinome Analysis
PMSF	phenylmethane sulfonyl fluoride
PRR	pattern recognition receptor
PRRSV	Porcine Reproductive and Respiratory Syndrome Virus
PVDF	polyvinylidene fluoride
RIPK	receptor-interacting serine-threonine kinases
SDS	sodium dodecyl sulphate
SLR	sequestosome 1-like receptor
SQSTM1	sequestosome-1
TBS	Tris-buffered saline
TEMED	tetramethylethylenediamine
TLR	toll-like receptor
ULK	unc-51-like kinase

Chapter 1: General Introduction

1.1 Autophagy

1.1.1 Introduction

Autophagy (a term coined in 1963 by Christian de Duve[1], in Greek meaning 'self-eating') is a complex process by which cells degrade intracellular, cytoplasmic components via a network of interconnected vacuoles, termed 'autophagosomes' and lysosomes, in order to carry out a variety of functions for the cell[2]. It is important to note the existence of several forms of autophagy, including microautophagy (direct engulfment by lytic vacuoles) and chaperone-mediated autophagy (a highly-selective form of autophagy), which are present in many cell types[3]. However, the focus of this manuscript is on the prototypical form of autophagy, termed macroautophagy (plainly referred to as autophagy henceforth). Autophagy is a ubiquitous and evolutionarily conserved process, present in all eukaryotic cells ranging from yeast[4], to plants[5,6], to modern mammals[7]. Many of the thirty-odd autophagy-regulating genes (termed Atgs) initially discovered in yeast have orthologs in other species, and some additional novel autophagy-associated genes in higher species have also been identified[7]. However, despite these minute differences in the molecular machinery present in the cell, the cellular autophagy pathway undergoes very similar stages in most species: membrane nucleation, membrane elongation, autophagosome maturation & closure, autophagosomal fusion with a lysosome generating an autophagolysosome, and degradation of vacuolar contents (Fig. 1-1)[7].

1.1.2 The autophagic machinery

The first step of the autophagy pathway is membrane nucleation or initiation. The source of membrane lipids in this step is still debated (as are many aspects of autophagy), with evidence

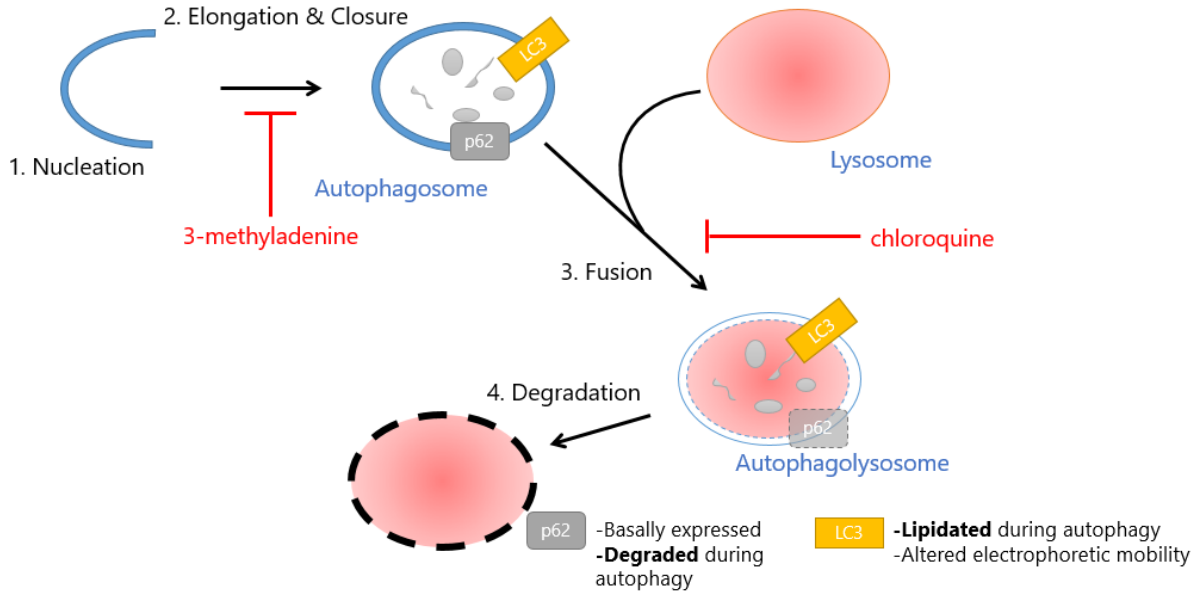

Figure 1-1. The general stages of the autophagy pathway in cells. Membrane nucleation is the first step, followed by membrane elongation and enclosure creating the autophagosome. The autophagosome then fuses with a hydrolytic enzyme-containing vacuole called a lysosome, forming an autophagolysosome. The contents of the autophagolysosome are subsequently degraded. Also shown are some early and late stage inhibitors of autophagy, 3-methyladenine and chloroquine, and some common protein markers of autophagy, namely p62 and LC3.

supporting both *de novo* generation and ER- as well as other organelle-derived lipid sourcing[8,9]. An 'isolation membrane' acts as a scaffold for various proteins that facilitate the elongation of the membrane, and eventual autophagosome formation. Key proteins at this stage, depicted in Figure 1-2, include: 1) the ubiquitin-like conjugating protein systems (one cluster involving ATG5, ATG12, and ATG16L and another involving MAP1LC3A (LC3-I) and the phospholipid phosphatidylethanolamine), 2) a class III phosphatidylinositol-3-phosphate kinase (also known as Vps34/PIK3C3) complex that produces lipid molecules and promotes autophagosome formation[10], and 3) regulatory kinases unc-51-like kinase (ULK) 1 and ULK2[9]. Several of these proteins, especially LC3-II (the lipidated form of LC3-I that is formed during autophagy) and sequestosome-1 (p62/SQSTM1) are widely used as autophagic markers.

1.1.3 The functions of autophagy

1.1.3.1 Maintenance of homeostasis

The cellular autophagy process was originally conceived as a mechanism for the regulation of homeostasis within the cell[1]. Basal levels of autophagy (as detected by various methods that will be described) can be measured in nearly all cell types. Interestingly, autophagy has been implicated as a major player in the cellular integrated stress response[11]. As such, increases in the levels of autophagy can be detected in cells subjected to stresses such as nutrient deprivation, growth factor depletion, hypoxia, reactive oxygen species, and others[11,12]. Nutrient deprivation can induce protein catabolism in the form of autophagy to produce amino acids that can then be converted into an energy source for the cell by gluconeogenesis[13]. In the heart, the autophagy pathway can play an important role in protecting against ischemic injury through the modulation of cell death pathways (described below)[14]. Reactive oxidative species and other oxidative

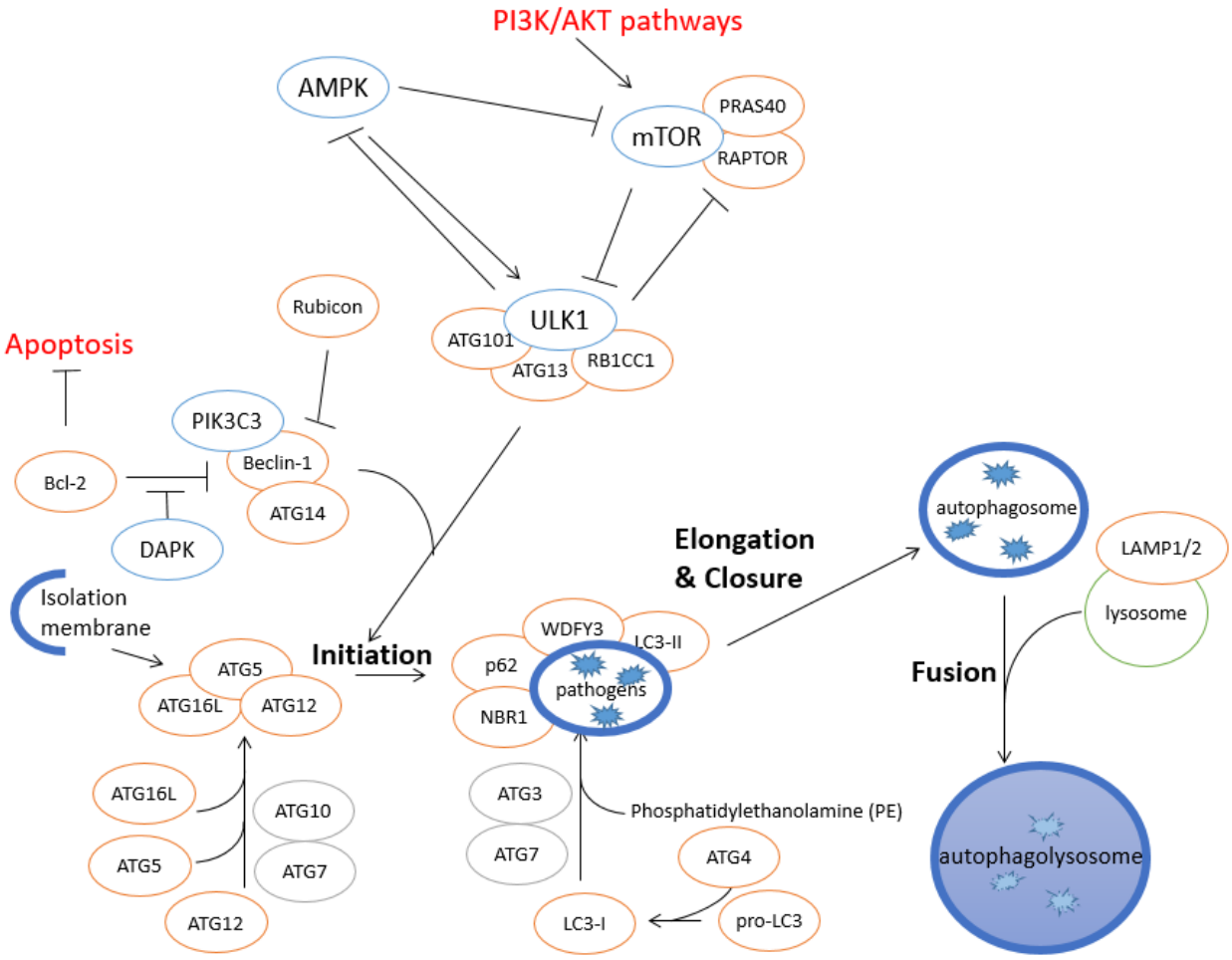

Figure 1-2. An overview of the key proteins involved in the autophagy cascade. Illustration reproduced with modifications courtesy of Cell Signaling Technology, Inc. (www.cellsignal.com).

stressors activate various intracellular signalling pathways that can activate autophagy such as those involving the mitogen-activated kinase (MAPK) and c-Jun N-terminal kinase 1 (JNK1) pathways[11]. Along the same lines, DNA damage can induce autophagy through the expression of the tumor suppressor protein p53 (which coincidentally has both pro- and anti-autophagic functions) and its responsive genes[11].

Another way that autophagy regulates cellular homeostasis is, in tandem with the proteasomal degradation pathway, through the control of unneeded, extraneous, and misfolded or mutated proteins[7]. Improper clearance of potentially toxic protein aggregates (due to the clearance machinery being overwhelmed or lacking the ability to take up such aggregates) can lead to numerous pathological states. An example of this function is the role of autophagy in the degradation (or lack thereof) of a mutated version of the protein α-synuclein in the brain, which has been implicated in the development of Parkinson's disease (PD) and other neurodegenerative disorders termed "α-synucleinopathies"[15]. Organelles can also be targets of autophagic degradation, as evidenced by the autophagy subroutine of selective degradation of defective or dysfunctional mitochondria (mitophagy), as a measure to avoid reactive oxygen species generation[16]. The impact of autophagy on cellular homeostasis is critical. However, autophagy also performs several other functions that are crucial for the survival of both the cell and the organism.

1.1.3.2 Fighting infection

The autophagy machinery is important for the protective functions of certain immune cells, a subject that has been extensively reviewed elsewhere[3]. One such function is the direct elimination of pathogens. Autophagy is initiated in response to recognition of pathogen-associated molecular

patterns (PAMPs) by certain pattern recognition receptors (PRRs) including toll-like (TLR) and nucleotide-binding oligomerization domain-like (NLR) receptors. Subsequent signalling events induce uptake of material into double-membraned (xenophagy) or single-membraned (LC3-associated phagocytosis; LAP) vacuoles, followed by delivery of antimicrobial peptides or the activation of the autophagic machinery leading to the degradation of vacuolar contents via fusion with a lysosome[3]. A third category of receptors, sequestosome-like receptors (SLRs), are capable of recognizing and targeting harmful cytoplasmic materials and initiating their elimination by physical recruitment of the autophagy machinery[3]. The importance of the autophagy pathway's ability to directly eliminate intracellular microorganisms is critical in phagocytic cells like monocytes and macrophages.

Another mechanism by which autophagy controls the immune response is through its modulation of inflammation. The inflammatory response involves the recruitment of immune cells to sites of injury for the purposes of propagation of the immune response and tissue repair[17]. This recruitment process is controlled by various cytokines and other molecules that influence the makeup of the inflammatory environment. The inflammasome, a cytoplasmic complex involving caspase 1, reacts to PAMPs and damage-associated molecular patterns (DAMPs) by processing and releasing pro-inflammatory cytokines such as IL-1β (an inducer of further inflammatory molecules like nitric oxide) and IL-18 (which induces Th1 cytokine production and enhances cell-mediated cytotoxicity)[18,19,3]. Autophagy can enhance acute inflammatory signalling by enhancing the delivery of PAMPs to endosomal TLRs, leading to interferon-α production[3]. Autophagy may also curtail chronic inflammation, as defects in critical autophagy genes are associated with inflammatory disorders such as Crohn's disease[3]. Conversely, autophagy can suppress inflammation by reducing inflammasome activation via clearance of inflammasome agonists using

its degradative machinery. The two-sided nature of this control emphasizes the importance of autophagy in inflammation, especially in cells of the innate immune system such as macrophages and dendritic cells.

One critically important process in the immune response is that of antigen presentation and subsequent T cell responses. Briefly, antigen presentation involves the engulfment of either intracellular or exogenous antigens, which are then degraded and presented on the surface of antigen-presenting cells (APCs), including dendritic cells and macrophages[20]. These APCs present the processed antigens to T cells, which along with costimulatory signals initiate the adaptive immune response. Autophagy works in tandem with the cellular proteasome to process proteins into peptide antigens for display on major histocompatibility complex (MHC) class II molecules, and through LC3-associated phagocytosis may contribute to MHC class I presentation as well[3]. In addition to their ability to influence T cell activation through antigen presentation, autophagy is also involved in maintaining T cell homeostasis and function[3].

1.1.3.3 Regulation of cell death

Recent studies show that autophagy can play a dual role in cell death, as both an antagonist and as an enabler[21]. However, this area is relatively understudied and some controversy remains[22]. It is clear that autophagy promotes the survival of cells through the mitigation of stress. However, under stress, it is possible that autophagy is induced in an attempt to mitigate said stress, and under conditions where the cell is unable to do so, it undergoes cell death. It is also possible that in some cases the typical machinery required for programmed cell death is insufficient, and the machinery for autophagy assists in some way[23]. Interestingly, the autophagy pathway has recently been ascribed a novel form of programmed cell death, which is described in further detail below.

1.2 Programmed cell death

1.2.1 Why do cells die?

The process of programmed cell death is, similarly to autophagy, a ubiquitously expressed and utilized, and tightly regulated, collection of pathways in nearly all cell types[24]. It may at first glance seem counterintuitive for cells to have a mechanism for enacting their own death. However, programmed cell death functions as an important mechanism for the control of growth and development as well as immunity in eukaryotes. For example, during mammalian growth, the nervous system generates an overabundance of cells, followed by the subsequent programmed cell death of those cells that do not establish effective synaptic connections[24]. During infection moreover, one of the body's most important methods for fighting infection is the ability to induce the death of infected cells, thus curtailing infection[24]. Much like autophagy, understanding how programmed cell death is regulated in a given disease model may be key to the identification of therapeutic targets. Additionally, physical or chemical injury to the cell can bring about cellular demise, but in a non-programmed manner[25].

1.2.2 Modes of programmed cell death

Programmed cell death (PCD) is distinguished from a non-programmed cell death, historically referred to as necrosis[25]. PCD often involves the induction of numerous signalling pathways in a stepwise manner, whereas necrosis involves almost an immediate cell death, often linked to a rapid loss of membrane integrity[25]. The distinction between programmed and non-programed is, however, being eroded, with the discovery of a type of programmed necrosis

(necroptosis) mediated by receptor-interacting serine-threonine kinases (RIPKs)[26]. Additionally, programmed cell death has been revealed to be broken down into numerous different subroutines, utilizing different signalling pathways and effector molecules, and engaging different physiological responses, but leading to the same conclusion: cellular demise. The proto-typical form of PCD, termed apoptosis, is normally mediated by a cleavage cascade involving a family of proteins termed caspases, or cysteine-aspartic proteases[24]. This type of cell death results in several notable phenotypic characterizations, including membrane phosphatidylserine externalization, membrane blebbing (while maintaining membrane integrity), and DNA fragmentation[24]. Apoptosis is typically divided into two categories: intrinsic (also known as the mitochondrial pathway) and extrinsic (also known as the death receptor pathway), with each being governed by a different set of initiating factors and caspases, but both leading to the same end result[24].

In addition to apoptosis, several other critical subroutines of cell death have been elucidated. Pyroptosis, for example, is a type of cell death associated with the inflammatory response and mediated by the caspase 1 protein, and is distinct from apoptosis[25]. In another example, cellular detachment of the extracellular matrix can cause anoikis, or cellular "death by neglect"[27].

1.2.3 Autophagic cell death

Autophagy was recently attributed to a novel form of cell death, termed autosis[22,28]. Autosis is a highly inducible and reproducible form of cell death that can be down-regulated with the knockout of important autophagy-regulatory genes[22]. Autosis can be induced by a novel autophagy-inducing peptide (Atg peptide) comprised of a section of amino acids from the autophagy-regulatory protein Beclin 1 and the cellular transducing portion of the Tat protein of

human immunodeficiency virus[22]. Cells undergoing autosis have distinct phenotypic characteristics. These include the early presence of autophagosomes followed by their disappearance in later stages, focal plasma membrane rupture, convolution and shrinkage of the nuclear membrane, ballooning of the perinuclear space, concavity of the nuclear surface, and abnormal mitochondria and ER[22]. Interestingly, a screen of potential autosis inhibitors implicated molecules referred to as cardiac glycosides, which inhibit the activity of cellular sodium-potassium ATPases[28]. This suggested the involvement of Na^+,K^+-ATPases in the mechanism of autosis.

It is unclear to date what role autosis may play in numerous autophagy- and cell-death-implicated pathologies. Several important diseases, including cancers, neurodegenerative disorders, and infectious and autoimmune disorders have been linked to the dysregulation of autophagy and programmed cell death[29]. This underlines the importance of tight regulation of both autophagy and programmed cell death, and the interaction between these processes.

Despite its ability to induce autosis in cells at relatively high concentrations, the autophagy-inducing peptide may have several potential therapeutic applications either by the induction of autophagy or cell death by autosis. For example, the peptide displayed an ability to reduce titres of certain positive-stranded RNA viruses both *in vitro* as well as *in vivo*[30].

1.3 Monocytes and macrophages

1.3.1 Importance in immunity

Monocytes and macrophages (M/Ms) represent a key segment of the innate immune system, which is the early, non-antigen-specific response to pathological agents[31,32]. The innate immune response is generally initiated via the recognition of the previously-described PAMPs,

motifs that are commonly conserved on pathogens and not found in higher eukaryotes. PAMPs are recognized by PRR expressed by innate immune cells including dendritic cells, M/Ms, and neutrophils[31,33]. Recognition of PAMPs by PRRs such as TLRs signals for the recruitment of adaptor molecules like MyD88, leading to the subsequent activation of transcription factors like NF-κB, which are responsible for inducing the expression of pro-inflammatory cytokines and the activation of inflammasomes[31]. This cellular response ensures that the milieu at the site of the infection or wound is ideal for the recruitment of immune cells to drive the immune response as well as tissue repair. In addition to cytokine secretion and immune response mobilization, M/Ms are involved in the direct degradation of harmful agents via phagocytosis, which as previously described involves vacuolization of harmful materials followed by recruitment of the autophagy machinery and lysosomal fusion[3].

M/Ms are also critical in the control of infection by mobilizing the adaptive immune system, the anemnestic and antigen-specific immune response. APCs such as dendritic cells and in some cases macrophages recognize PAMPs through their PRRs as previously described. Extracellular pathogenic proteins are degraded and processed into peptide antigens, which are presented on MHC class II molecules on the cell surface[20]. Following migration to the lymph nodes and the display of peptide antigens in conjunction with MHC class II and other co-stimulatory signals on the DC surface, the cells communicate with and activate $CD4^+$ T helper cells, which produce "helper" cytokines that drive the adaptive immune response. Similarly, MHC class I molecules display mainly endogenously processed antigens, including self- and pathogen-specific peptide antigens, on all non-nucleated cells. These can then be probed and foreign antigens are targeted by $CD8^+$ cytotoxic T cells, leading to the elimination of the infected cell[34].

1.3.2 Regulation of M/Ms function

Due to their importance in both the innate and adaptive arms of the immune system, tight regulation of M/M function is critical for the host to eliminate and survive infection. Furthermore, the failure to control and downregulate an immune response once infection is cleared can be just as damaging as an inadequate immune response to the invading pathogen. Several mechanisms exist to control both the up- and down-regulation of M/M functions. Monocytes are the precursors for most phenotypes of macrophages, and differentiate into macrophages in the tissues in response to the signals at the damaged site[35]. Due to the potential differences in macrophage function following differentiation, a paradigm has been proposed to describe the different avenues of macrophage activation, termed classic (M1) and alternative (M2)[36]. Classic activation of macrophages occurs in response to stimulation with IFNγ, lipopolysaccharides, virus particles or granulocyte macrophage colony-stimulating factor (GM-CSF), and occurs as a precursor to proto-typical Th1 immune responses, including inflammation and the killing of intracellular pathogens[36]. Alternative activation is stimulated by IL-4, IgG, IL-10, and macrophage colony-stimulating factor (M-CSF), and can be subdivided into three subtypes: M2a, facilitating allergy and parasitic immune responses, M2b, facilitating immunoregulation via crosstalk with B cells, and M2c, facilitating tissue remodelling and repair[36]. While this paradigm is useful in classifying different types of macrophage activation in response to differing types of disease, the *in vivo* make up of activated macrophages is likely fluid and thus should not be constrained too narrowly.

In addition to the regulation of M/Ms by cytokines, other compounds can also affect the potency of M/Ms. For example, inducing autophagy in M/Ms using the pharmaceutical drug rapamycin can often stimulate their anti-microbial potential, leading to faster clearance of infection[37]. However, this type of M/M regulation can also be hijacked by pathogens. For example,

the Porcine Reproductive and Respiratory Syndrome Virus (PRRSV) may exploit the autophagy pathway to enhance its replication[38].

1.4 Cellular signalling by protein phosphorylation

Cellular signalling by protein phosphorylation is one of the major forms of signalling carried out by all types of cells, and is separate from other forms such as ubiquitination or ion binding. In eukaryotes, the large majority of phosphorylation events occur on the hydroxyl-containing amino acids: serine, threonine, and tyrosine[39]. These amino acid residues act as a substrate for protein kinases, which reversibly attach a phosphate group, sourced from ATP, to the free hydroxyl of the amino acid[39]. Binding of the phosphate group can induce a number of protein changes, often in protein conformation and/or protein polarity, and modulate protein-protein interactions to propagate intracellular signalling. Attached phosphate groups can also be removed, by protein phosphatases, to downregulate the effect[39]. Thus, both protein phosphorylation and dephosphorylation are critical events in cellular signalling. Individual phosphorylation events are often part of a larger phosphorylation cascade, in which an initial signal can be transduced through multiple signalling proteins via subsequent phosphorylation events[39]. These types of signalling cascades, due to their importance in cell survival, are tightly controlled and highly complex, and our understanding of many of these pathways is incomplete.

Kinome microarray analysis represents a large step forward in our approach to better understand cellular signalling events in a high-throughput manner, *in silico* (Fig. 1-3)[40]. Following the principle used for genetic microarrays, kinome microarrays include numerous peptides attached to a solid support in a grid-like format. These peptides represent the phosphorylation

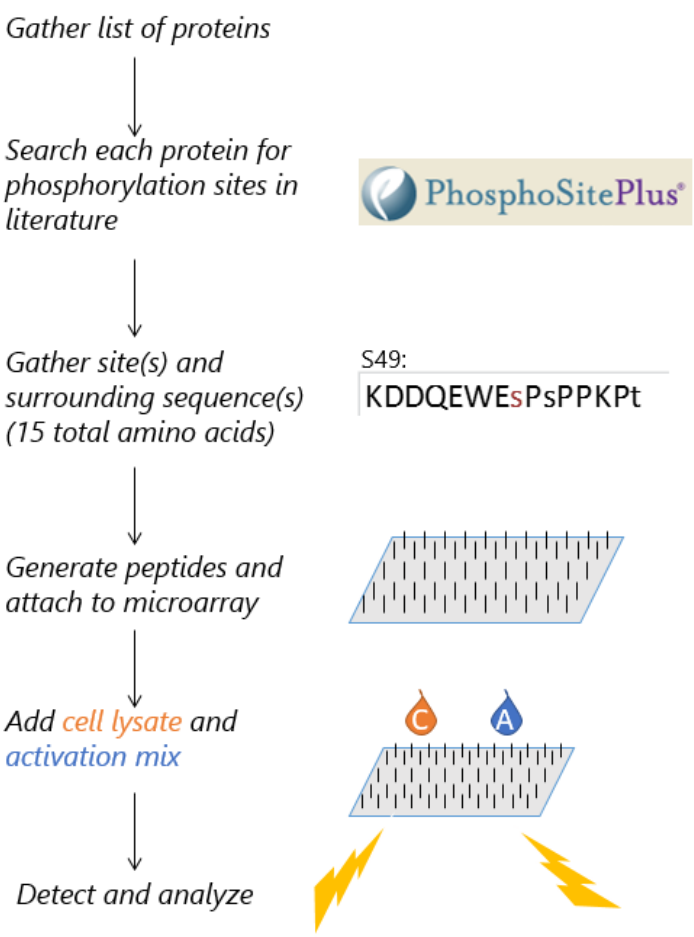

Figure 1-3. A general overview of the kinome microarray design and analysis protocol. A list of proteins of interest is gathered and key protein phosphorylations are assembled from the literature via the database phosphosite.org[41]. The 15 amino acid sequences (seven amino acids on each side of the phosphorylated residue) are generated and attached to a solid support. Cell lysates are generated and incubated on the microarray along with an activation mix containing ATP. Arrays are then incubated with a phospho-protein stain and fluorescence is detected, followed by analysis of the identity of phosphorylated peptides and signal intensity.

sites of proteins of interest, usually a 15 amino acid sequence in which the eighth amino acid is the phosphorylated residue. The peptides can be chosen to represent a broad array of signalling proteins for use as a screening tool or be more fine-tuned to specific pathways, and are used to detect the phosphorylation cascades that occur in response to a given cell stimulus. Arrays are incubated with stimulated cell lysates that contain cellular kinases, proteins that phosphorylate other proteins. These kinases phosphorylate the peptides on the microarray, which are then detected using a phospho-stain and analyzed. On the whole, kinome arrays thus allow experimenters to examine the signalling capacity of the cell in response to different treatments.

This technology, despite its novelty, has already been advanced in several ways since its inception. It can be expanded to species that do not have commonly available phosphorylation data via prediction of conserved peptide sequences[42,43,44]. Additionally, specifically-tailored tools for analyzing kinome data have been developed[45]. We thus opted to use kinome microarray analysis to enhance our understanding of the molecular mechanisms of monocyte cell death.

Chapter 2: Thesis Rationale and Objectives

In addition to the M1-defining, anti-microbial inductive capacity of IFNγ, this important cytokine also plays other roles. We have previously found that IFNγ stimulation of monocytes also induced death in these cells, which may function as a regulatory mechanism in controlling the immune response (Fig. 2-1A)[46]. In contrast, monocytes stimulated with IL-10, an M2-defining and immunoregulatory cytokine, curtails both spontaneous and IFNγ-induced cell death (Fig. 2-1A)[47]. Furthermore, we found that spontaneous and IFNγ-induced cell death was caspase-independent, but rather involved the autophagy pathway and could be reduced by inhibiting autophagy (Fig. 2-1B)[47]. Interestingly, the pro-survival effects of IL-10 were also associated with the autophagy pathway[47]. Therefore, our laboratory is interested in understanding the molecular mechanisms responsible for the dual role of autophagy in monocytic cell death. We are also investigating the anti-microbial capacity of the Atg peptide mentioned above, a peptide that has been shown recently to induce autophagic cell death[28]. As a result, I aimed to develop and evaluate a kinome array approach for the further study of monocyte autophagic cell death with the following specific objectives.

1. Establish an *in vitro* model to study the regulation of programmed cell death in monocytic cells

2. Design and test a kinome-based approach to investigate the molecular mechanisms associated with autophagic cell death in monocytic cells

    i. Designing the kinome array

    ii. Analyzing the array data

3. Validate kinome array results by Western blotting

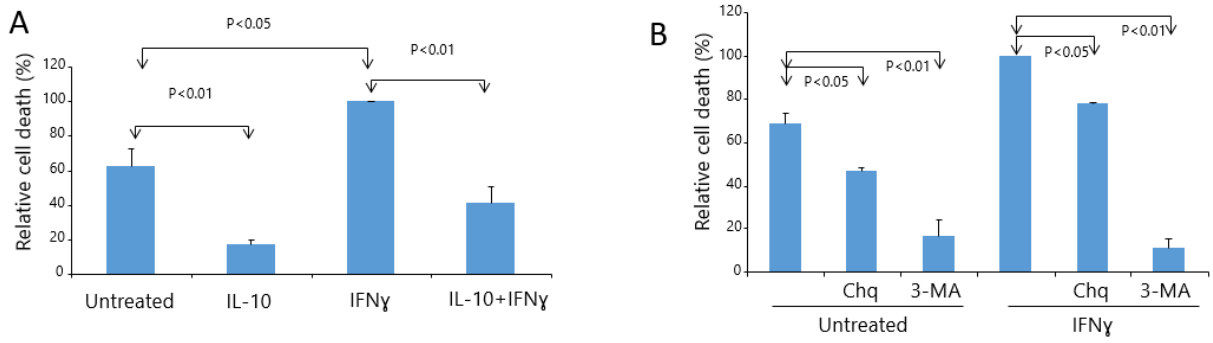

Figure 2-1. Relative cell death of monocytes in response to IFNγ and IL-10 treatment. Flow cytometric analysis of cell death in human monocytes A) stimulated with 10 ng/mL IFNγ and/or IL-10, and B) in monocytes pre-treated with the autophagy inhibitors Chloroquine (Chq; average of 6.25 to 25 µM) and 3-methyladenine (3-MA; average of 5 to 10 µM) followed by stimulation with 10 ng/mL IFNγ[47].

Chapter 3: Materials and Methods

3.1 Isolation of monocytes from human peripheral blood mononuclear cells

Following University of Saskatchewan Ethics Board approval, between 200 and 250 mL of blood were collected from each volunteer blood donor by peripheral venipuncture (TLC Mobile Lab, Saskatoon, SK, CA). Blood was mixed with an equal volume of sterile phosphate-buffered saline (PBS; Sigma-Aldrich, St. Louis, MI, USA), and approximately 37 mL of this mixture was layered over 12 mL of Ficoll-Paque Plus (GE Healthcare Bio-Sciences, Pittsburgh, PA, USA). The layered blood was centrifuged at 400 *x g* for 45 minutes without applying centrifuge brake. The resulting buffy coat containing peripheral blood mononuclear cells (PBMCs) was extracted and washed twice in sterile PBS. PBMCs were counted and monocytes were isolated by either positive or negative selection using Miltenyi Biotec CD14 Microbeads or the Pan Monocyte Isolation Kit, respectively, as recommended by the manufacturer (Miltenyi Biotec, Auburn, CA, USA). Briefly, for positive selection, PBMCs were resuspended in magnetic activated cell sorting (MACS) buffer supplied by the manufacturer, and 20 µL anti-CD14-conjugated microbeads were added per 10^7 cells. The mixture was incubated in the dark at 4 °C for 15 minutes. To wet the separating column, 3 mL of MACS buffer were added. Cells were washed in MACS buffer, then centrifuged at 300 *x g* for 10 minutes, and then resuspended in a final volume of 500 µL of MACs buffer. The suspension was added to the column with the magnet applied, and the flow-through fraction was discarded. With the magnet still applied, the column was washed three times with MACS buffer. Finally, the column was removed from the magnet and 5 mL of MACS buffer was added. The plunger was used to push the remaining monocyte-enriched cell fractions into a fresh tube. Cells were then counted and subsequently cultured.

For negative selection, PBMCs were resuspended in MACS buffer, and 10 µL FcR Blocking Reagent and 10 µL Biotin-Antibody Cocktail were added per 10^7 cells. The mixture was incubated in the dark at 4 °C for 5 minutes. 30 µL of MACS buffer was then added, followed by 20 µL of Anti-Biotin Microbeads per 10^7 cells and subsequent incubation in the dark at 4 °C for 10 minutes. The separating column was pre-wet with 3 mL of MACS buffer. Cells were resuspended in a volume of 500 µL of MACS buffer, and with the magnet applied the suspension was added to the column. The flow-through, containing the monocyte-enriched fraction, was collected and the column, with the magnet still applied, was washed three times with MACS buffer and combined with the previous flow-through. Cells were then counted and subsequently cultured.

3.2 Culture of human monocytes and the U937 monocytic cell line

After isolation, human monocytes or U937 monocytic cells (American Type Culture Collection, Manassas, VA, USA) were cultured in RPMI 1640 (GE Healthcare) supplemented with 10% fetal bovine serum (FBS; GE Healthcare), 1% sodium pyruvate, 1% β-mercaptoethanol (Sigma-Aldrich), and 10 U/mL Penicillin-Streptomycin (PenStrep; Life Technologies, Carlsbad, CA, USA). Cells were incubated to 1 x 10^6 cells/mL at 37 °C and 5% CO_2.

3.3 Flow cytometric analysis of purity of monocyte cultures

After isolation, human monocytes were fixed in 2% paraformaldehyde for 10 minutes at 4 °C. The cells were then washed in 0.1% bovine serum albumin (BSA; Sigma-Aldrich)/PBS containing buffer, followed by resuspension at a final volume of 100 µL. 20 µL of mouse anti-human $CD14^+$-PE or mouse IgG1-PE isotype control (ThermoFisher Scientific, Waltham, MA,

USA) antibodies (Abs) were added and incubated for 15 minutes at room temperature. Cells were washed once more in 0.1% BSA/PBS buffer, then resuspended in 2% paraformaldehyde until analysis. Samples were analyzed using a BD FACSCalibur flow cytometer (BD Biosciences, San Jose, CA, USA) and the FlowJo analysis software (FlowJo, LLC, Ashland, OR, USA).

3.4 Cell stimulations

For the quantification of cell death, 5 x 10^5 U937 monocytic cells or isolated primary human monocytes were rested in fresh media for 1 hr. This was followed by cell stimulation with 5, 15, and 30 µM (for U937 cells) or 2.5 µM (for primary monocytes) of autophagic cell death-inducing peptide (Atg peptide), or 30 µM of a scrambled sequence (Control) peptide (both Atg peptide and Control peptide kindly provided by Dr. Beth Levine, Howard Hughes Medical Center, University of Texas Southwestern) or cells were left untreated overnight at 37 °C and 5% CO_2. 1 µM staurosporine (Sigma-Aldrich) stimulation overnight was used as a positive control for cell death[48].

For the kinome analysis, 25 x 10^6 U937 monocytic cells were rested in fresh media for 1 hr, followed by stimulation with 30 µM of Atg peptide, Control peptide or left untreated for 15 min or 1 hr at 37 °C and 5% CO_2. Two replicate experiments were performed.

For Western blots, 4 x 10^6 U937 monocytic cells were rested in fresh media for 1 hr, followed by stimulation with 30 µM of Atg peptide, Control peptide or left untreated for 15 min or 1 hr at 37 °C and 5% CO_2.

3.5 Quantification of cell death by flow cytometry

Cell death following the various stimulations was quantified using the Alexa Fluor® 488 Annexin V/Dead Cell Apoptosis Kit (ThermoFisher Scientific) according to the manufacturer's instructions. Briefly, 5 x 10^5 cells were washed twice in PBS, followed by resuspension in 100 µL of annexin binding buffer (10 mM HEPES, 140 mM NaCl, 2.5 mM $CaCl_2$, pH 7.4). 5 µL of Annexin V-488 conjugate and 1 µL of 100 µg/ml propidium iodide (PI) were added, followed by a 15 min incubation period at room temperature. 400 µL of annexin binding buffer were added and cells were kept on ice until detection on a flow cytometer. Dead cells were quantified by calculating the percentage of Annexin V-488^+/PI^+ cells. Samples were analyzed using a BD FACSCalibur flow cytometer and FlowJo analysis software.

3.6 Cellular protein extraction and quantification

Cell pellets of 4 x 10^6 or 10 x 10^6 cells were kept on ice and washed once in PBS, followed by resuspension in protein extraction buffer (10 mM Tris, pH 8, 50 mM NaCl, 2 mM EDTA, 1 mM EGTA, 1% Triton X-100, 50 mM NaF, 1 mM Na_3VO_4, 1 mM PMSF, 1X cOmplete Mini Protease Inhibitor Cocktail Tablet™ (Roche Life Science, Laval, QC, CA) for Western blotting or kinome extraction buffer (20 mM Tris, pH 8, 150 mM NaCl, 1 mM EDTA, 1 mM EGTA, 1% Triton X-100 (Sigma-Aldrich), 2.5 mM sodium pyrophosphate, 1 mM Na_3VO_4, 1mM NaF, 1 mM PMSF, 1 µg/mL aprotinin (Sigma-Aldrich), 1 µg/mL leupeptin (Sigma-Aldrich)) for kinome analysis. This suspension was centrifuged at 20 000 *x g* for 20 minutes and the protein-containing supernatant transferred to a separate tube. Proteins were quantified with the Bradford method[49] using a Bio-Rad Protein Quantification Kit (Bio-Rad, Hercules, CA, USA). Briefly, working dye

reagent was prepared by adding 4 parts ddH_2O to 1 part stock dye concentrate. Proteins were diluted 1:10 in ddH_2O and 10 µL diluted protein added to 200 µL working dye reagent. The solution was incubated at room temperature for 5 minutes and then analyzed using a spectrophotometer at 595 nm. Sample protein concentrations were interpolated from a standard curve generated using serial dilutions of a known quantity of BSA protein.

3.7 Western blotting

Polyacrylamide gels were prepared (Resolving gel: 14% bis-acrylamide (Sigma-Aldrich), 0.39 mM Tris pH 7.4, 0.1% (w/v) sodium dodecyl sulphate (SDS), 1 µg/ml ammonium persulphate (APS), and 0.1% (v/v) tetramethylethylenediamine (TEMED); Stacking gel: 6.5% bis-acrylamide, 0.14M Tris-HCL pH 6.8, 0.11% (w/v) SDS, 1 µg/ml APS, 0.11% (v/v) TEMED) and 60 µg protein samples were loaded. Gels were electrophoresed at 150 V for 2 hours, or until the dye front migrated out of the gel. Proteins were wet transferred onto polyvinylidene fluoride (PVDF; ThermoFisher Scientific) membranes at 300 mA for 1 hour. Membranes were blocked in 5% BSA/PBS for LC3-II and p62 expression or 5% BSA/Tris Buffered Saline (TBS) for phosphoprotein expression overnight at 4 °C or for 1 hour at room temperature, respectively. Membranes were washed three times in PBS-0.1% Tween (PBST) and probed for LC3 and p62 expression or TBS-0.1% Tween (TBST) for phosphoprotein expression and then incubated with primary antibody (anti-p62 at 1:1000; anti-GAPDH at 1:2000; anti-β-actin at 1:2000; anti-Phospho(Ser136)-Bad at 1:500; anti-Bad at 1:500; anti-Phospho(Ser9)-p53 at 1:500; anti-p53 at 1:500; anti-Phospho(Y10)-ATP1A1 at 1:500; antanci-ATP1A1 at 1:500; anti-Phospho(Ser65)-4E-BP1 at 1:500; anti-4E-BP1 at 1:500 (Cell Signaling Technologies, Danvers, MA, USA)) in the appropriate blocking solution for 90 minutes at room temperature or overnight at 4°C. This was

followed by three more washes in PBST and subsequent incubation with secondary antibody (anti-Rabbit Cy5; anti-Rabbit Cy3; anti-Mouse Cy3 (Cell Signalling Technologies)) at a dilution of 1:2500 in PBST or TBST for 1 hour. Finally, the membrane was washed three times in PBST or TBST and three times in PBS or TBS, and allowed to dry overnight in the absence of light. Membranes were imaged using a Bio-Rad VersaDoc. Western blot images and detected band intensities were analyzed using the Bio-Rad Image Lab Software. Band intensity values were extracted into Microsoft Excel and protein of interest intensities were compared to housekeeping protein intensities to generate a ratio of protein expression.

3.8 Kinome analysis

3.8.1 Kinome array design & production

To design the kinome array, proteins involved in the autophagic machinery, typical apoptotic proteins, alternative forms of cell death like necroptosis, as well as key upstream signalling molecules, were chosen via a thorough search and review of the literature (Fig. 3-1). From this generated list of key proteins, their respective phosphorylation sites were identified based on the presence of records from the literature referenced on the phosphosite.org website[41]. Identified sites were chosen based on the use of site-specific experimental methods to establish protein function, and relevance of the function to autophagy and/or cell death. The chosen phosphorylation site 15 amino acid sequences (7 amino acids on either side of the phosphorylated residue) were recorded. In total, 298 unique peptide sequences were chosen (Table 3-1), and sent to JPT Peptide Technologies (Berlin, Germany) for synthesis and array production. Each array contained 3 technical replicates per selected peptide.

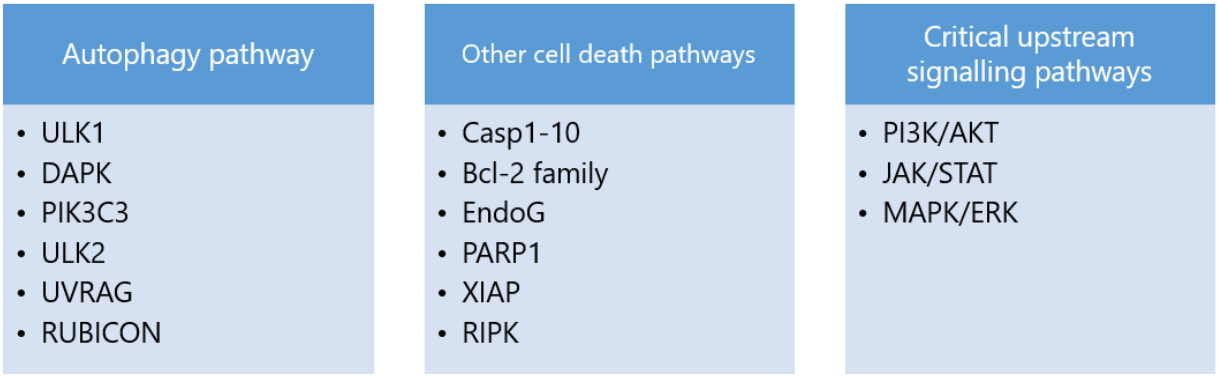

Figure 3-1. A sampling of proteins and signalling pathways represented on our custom kinome array.

Table 3-1. A list of the proteins and their associated phosphorylation sites represented on the autophagy- and cell-death-specific kinome array

Protein	Phosphorylation Sites											
DAP	S3	S49	S51									
DAP3	S215	T216	S220	T237	S251	S252	S280					
DAPK1	S289	S308	S333	S734								
DAPK2	S299	S318	S349	S367	S368							
DAPK3	T180	T225	T265	T299	T306	S311						
PRAS40	S183	S221	T246									
PIK3C3	T159	S244	T668									
PIK3R4	S865											
ULK1	S467	S556	S638	S758								
ATG13	S355	S361										
RB1CC1	S222	S243	S257									
ATG101	Y164											
ATG4B	S383											
ATG3	Y18											
ATG5	T75											
ATG16L	S269											
LC3A	S12											
LC3B	T6	T29										
ATG2B	Y264	T398										
ATG9A	S14	S18	S656	S735	S738	S741	S759	S761	S828			
FAM48A	T494											
STX17	Y157	S289										
beclin 1	S15	S90	S93	T108	T119	Y229	Y233	S234	S295	Y352		
UVRAG	S498	T518	Y681	S689	S696	S697						
SH3GLB1	Y80	T145										
AMBRA1	S52	S639	S696									
VMP1	Y224											
Bcl-2	T56	T69	S70	T74	S87							
Bcl-xL	T47	S49	S62	T115								
SQSTM1	S24	S207	T269	T272	S332	S349	S366	S403				
WDFY3	T818	S2278	S3335	S3339								
TFEB	S142	S211										
FOXO3A	T32	S90	T179	S209	S215	S231	S232	S243	S253	S284	S294	S315
FOXO3A	S318	S321	S344	S399	S413	S425	T427	S555	S574	S588	S626	S644
mTOR	S1261	S2159	T2164	T2446	S2448	S2454	T2473	T2474	S2478	S2481		
Deptor	S244	S265	S286	S287	S291	T295	S299					
LST8	S43											
RAPTOR	S696	T706	S722	S792	S859	S863	S877					
rictor	T1135											
AMPKA1	T183	S496										
AMPKA2	T172											
AMPKB2	S24	S108	S182									
TAX1BP1	S666											
IKKA	T23	S176	S180									
IKKB	S177	S181	Y199	S740	S750							
IKKE	S172											
IKK-g	S68	S85		S376								
TAB2	S372	S419										
STAT6	Y641											

Table 3-1, continued.

Protein	Phosphorylation Sites												
STAT3	Y705	S727											
Akt1	T72	S124	S129	S246	T308	T450	S473						
Akt2	T309	S474											
Akt3	T305	S472											
EIF2a	S52												
EIF2b	S2												
JNK1	T183	Y185											
TAK1	T184	T187	S439										
TBK1	S172												
Bad	S75	S99	S118	S134									
Bax	S163	T167											
p38a	T180	Y182											
RIPK2	S176												
JAK1	Y1034	Y1035											
JAK2	Y221	Y570	Y813	Y1007	Y1008								
STAT1	Y701	S727											
TYK2	Y1054	Y1055											
iNOS	S745												
Met	Y1234												
MSK2	S360												
PPARg	S112												
SMAD3	S416												
PI3K p85 subunit β	Y464												
Bim	S69												
CHOP	S79												
IKK-alpha	S473												
MK3	Y187												
$p27^{kip1}$	Y74												
PDK1	Y373												
Casp1	S376												
Casp2	S139	S157	S340										
Casp3	S150												
Casp6	S257												
Casp7	S30	T173	S239										
Casp8	Y380	S387	T448										
Casp9	T125	S144	Y153	S183	S196								
ATP1A1	Y10	S16	Y55	Y260	Y542	Y684	S943						
PPP2CA	T304	Y307											
PARP1	S372	T373											
RhoA	S188												
ROCK1	S1333												
ROCK2	Y722	S1366											
p53	S6	S9	S15	T18	S20	S33	S37	S46	T55	T81	S269	T284	S315	S392
p73	T86	Y99											
XIAP	S87												
Drp1	S616	S637											
VAMP7	Y45												
Mcl-1	S64	T92	S121	S159	T163								
4E-BP1	T37	T46	S65	T70									
ERK1	T202	T204											
ERK2	T185	Y187											

3.8.2 Kinome analysis protocol

Kinome analysis was performed as previously described with some modifications[42]. Two biological replicates per treatment were used. Briefly, 10 x 10^6 cells were lysed in 100 µL of Kinome Lysis Buffer (1µg/mL Aprotinin, 1 mM EDTA, 1 mM EGTA, 150 mM NaCl, 1 mM NaF, 1 mM Na_3VO_4, 1µg/mL Leupeptin, 1 mM PMSF, 20 mM Tris-HCl pH 7.5, 1% Triton, 2.5 mM sodium pyrophosphate) and incubated on ice for 10 minutes, followed by centrifugation at 14000 *x g* at 4 °C for 10 minutes. 70 µL of cellular lysate was mixed with 10 µL of Activation Mix (500 µM ATP, 0.05% v/v Brij-35, 0.25 mg/ml BSA, 50 mM $MgCl_2$, 50% glycerol) and incubated on a microarray for 2 hours at 37 °C. The microarray was then washed and incubated in ProQ Diamond Phosphoprotein Stain (ThermoFisher Scientific) with agitation for 1 hour, followed by three destaining washes (20% acetonitrile, 50 mM sodium acetate at pH 4.0) and a final wash in distilled H_2O. The arrays were allowed to dry and scanned at 532 to 560 nm using a GENEPIX 4200A microarray scanner (Molecular Devices, Sunnyvale, CA, USA), and analyzed using the GENEPIX 6.0 software.

Relative phosphorylation of peptides was calculated using PIIKA software[45]. Briefly, raw intensity data was extracted from GENEPIX 6.0 in Microsoft Excel. Raw intensities were organized according to PIIKA specifications and entered into PIIKA[45]. Treatment-treatment variability analysis using t tests provided differentially phosphorylated peptides, which were then filtered and visualized by significance and fold-change (FC).

Chapter 4: Results

4.1 Objective 1: Establish an in vitro model to study the regulation of programmed cell death in monocytic cells

4.1.1 Purity of peripheral blood mononuclear cells and isolated human monocytes

Our laboratory is interested in elucidating the molecular mechanisms responsible for programmed cell death in human monocytes. Therefore, my first objective was to establish an *in vitro* model to enable the further study of monocytic cell death. Primary human monocytes were isolated from the peripheral blood of human volunteers by positive and negative selection techniques. The purity of monocyte isolations was subsequently evaluated by staining with anti-CD14 antibodies (Abs) and flow cytometric analysis. Positive selection returned over 90% monocyte purity and negative selection returned approximately 70% purity (Fig. 4-1). Due to this higher purity, positive selection of monocytes was used for all subsequent experiments involving primary cells.

4.1.2 Autophagic cell death in primary human monocytes

As mentioned above, previous studies in the laboratory have found contrasting effects on monocytic cell death by the cytokines IFNγ and IL-10[47]. IFNγ is capable of inducing cell death in monocytes, while IL-10 exerts a protective effect against both IFNγ-induced and spontaneous monocytic cell death. Interestingly, both of these effects were found to be caspase-independent, and instead involved the autophagy pathway. Interesting also was the observation of the effects of the Atg peptide, capable of inducing autophagic cell death in numerous models[30]. Therefore, I evaluated the capacity of the Atg peptide to induce autophagic cell death in primary human monocytes (Figure 4-2A). Monocyte cell death was found to occur in response to a 2.5 μM

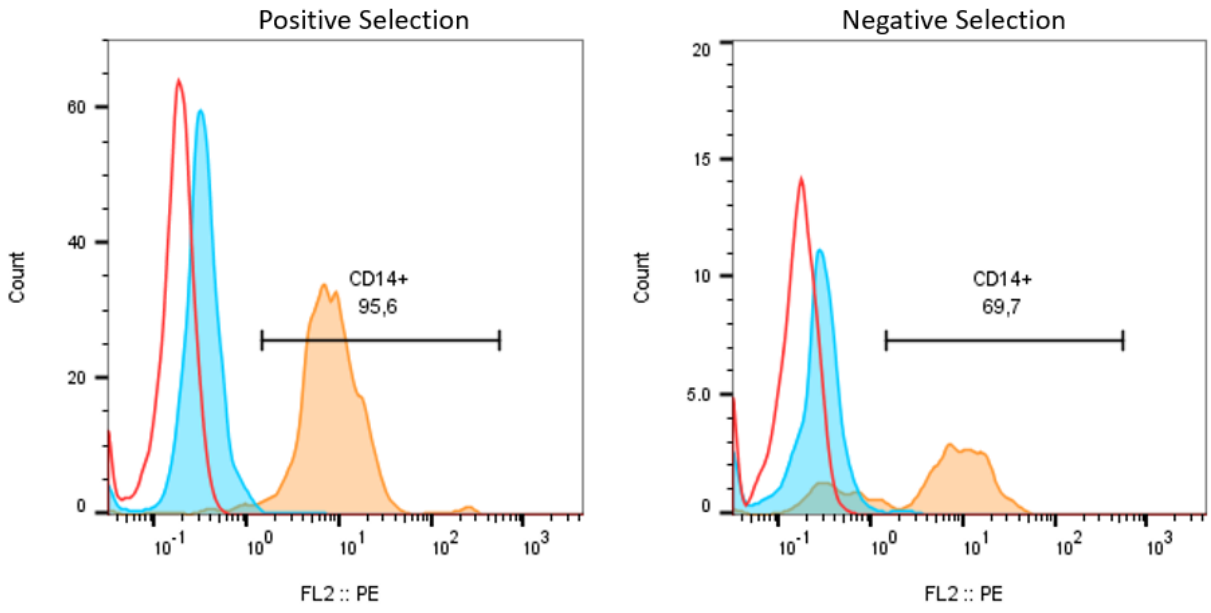

	Sample	% CD14⁺
	Unstimulated	0
	IgG1	1.49
	CD14	95.6

	Sample	% CD14⁺
	Unstimulated	0.30
	IgG1	1.88
	CD14	69.7

Figure 4-1. Flow cytometry analysis of human monocytes isolated from peripheral blood mononuclear cells using either positive or negative selection. $CD14^+$ antibodies were used to detect the monocyte population, mouse IgG1 was used as a negative control.

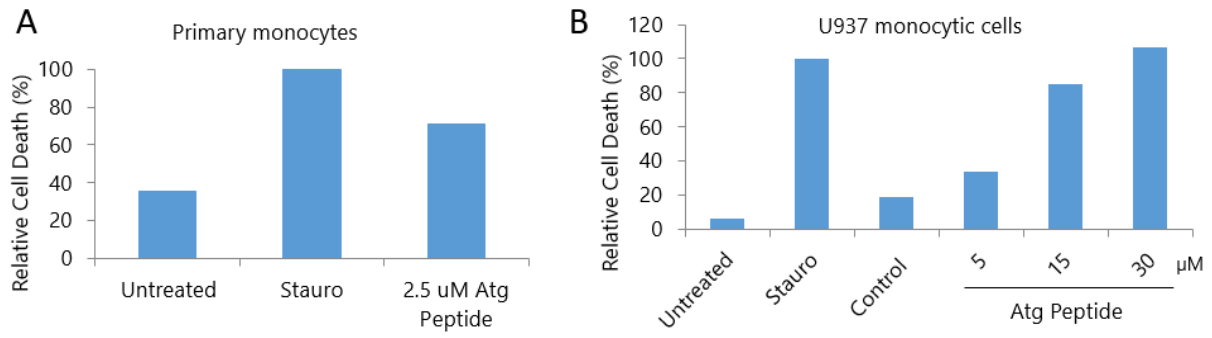

Figure 4-2. Relative cell death of monocytes or monocytic cells in response to Atg peptide treatment. Primary human monocytes (A) or U937 cells (B) were stimulated overnight with an autophagic cell death-inducing peptide (Atg peptide). 1 μM Staurosporine (Stauro) was used as a positive control for cell death. A scrambled peptide sequence (Control; 30 μM) was used as a negative control. Cells were then collected, stained with propidium iodide and analyzed using flow cytometry to detect programmed cell death. Cell death is shown as % relative to the sample exhibiting the highest induction (Relative Cell Death), ie. Staurosporine in (A) and 30 uM Atg Peptide in (B). One representative experiment each among greater than three conducted.

concentration of Atg peptide, roughly doubling the relative cell death of untreated cells and nearing the levels observed for the potent inducer of cell death Staurosporine[48], used as a positive control.

4.1.3 Autophagic cell death in a monocytic model cell line

In addition to primary monocytes, the U937 cell line is commonly used as an *in vitro* model human monocytic cell system. Therefore, I evaluated the effect of the Atg peptide on cell death in U937 cells (Figure 4-2B). The level of autophagic cell death detected rose with increasing concentrations of the Atg peptide from 5 to 30 µM, even exceeding those found in the positive control Staurosporine at the highest concentration. In contrast, cell death was not appreciably increased at the highest concentration (30 µM) of Control peptide.

4.2 Objective 2: Design and test a kinome-based approach to investigate the molecular mechanisms associated with autophagic cell death in monocytic cells

Having found that the Atg peptide potently induced cell death in both primary monocytes and the U937 monocytic cell line, the focus of my project turned to the design of a kinome microarray approach to study this phenomenon in greater detail. Kinome analysis would allow the identification of the potential signalling events that may be responsible for Atg peptide-induced autophagic cell death. It would also provide our laboratory with a powerful new tool to further investigate the dual role of the autophagy pathway in controlling cell death or survival, an example being the opposing death versus survival effects associated with IFNγ and IL-10, respectively, in monocytes. Thus, I proceeded to design a custom, autophagy-centric array, as described in section

3.8.1 above. Subsequently, the kinome array was synthesized and evaluated in the Atg peptide-treated monocytic cell model.

4.2.2 Kinome analysis of Atg-peptide stimulated monocytic cells

Due to the high number of cells required to attain sufficient protein concentrations for kinome analysis, as well as their relative ease of manipulation, I elected to use the U937 monocytic cell line rather than primary monocytes to initially evaluate our autophagy kinome arrays. U937 cells were treated with 30 μM Atg peptide or Control peptide or left untreated for 15 minutes and 1 hour. These time points were selected as a starting point, to detect both early and more distal signalling events in response to Atg peptide stimulation using this approach.

Overall, as depicted pictorially in Figures 4-3 and 4-4 by a visualization scheme and hierarchical clustering, respectively, the results show substantial phosphorylation differences between treatments for both 15 min and 1 hr. In Figure 4-3, data for peptides exhibiting similar levels of phosphorylation in response to Atg peptide versus control peptide are represented as symbols with homogeneous colouring. Peptides represented on the array that were differentially phosphorylated are depicted with symbols of heterogeneous colours, with yellow indicating increased phosphorylation compared to untreated control cells, and blue colouring indicating decreased phosphorylation. The relative degree of (de)phosphorylation corresponds with the intensity of the colour. Figure 4-4 demonstrates the hierarchical clustering of peptide phosphorylation status in response to treatments. Again, it appears that on the whole, the Atg peptide alters phosphorylation status appreciably more than control peptide, as compared to untreated samples. This is reflected by the relative distances between treatments in the upper dendrogram (Fig. 4-4A). Additionally, peptides with significant differential phosphorylation

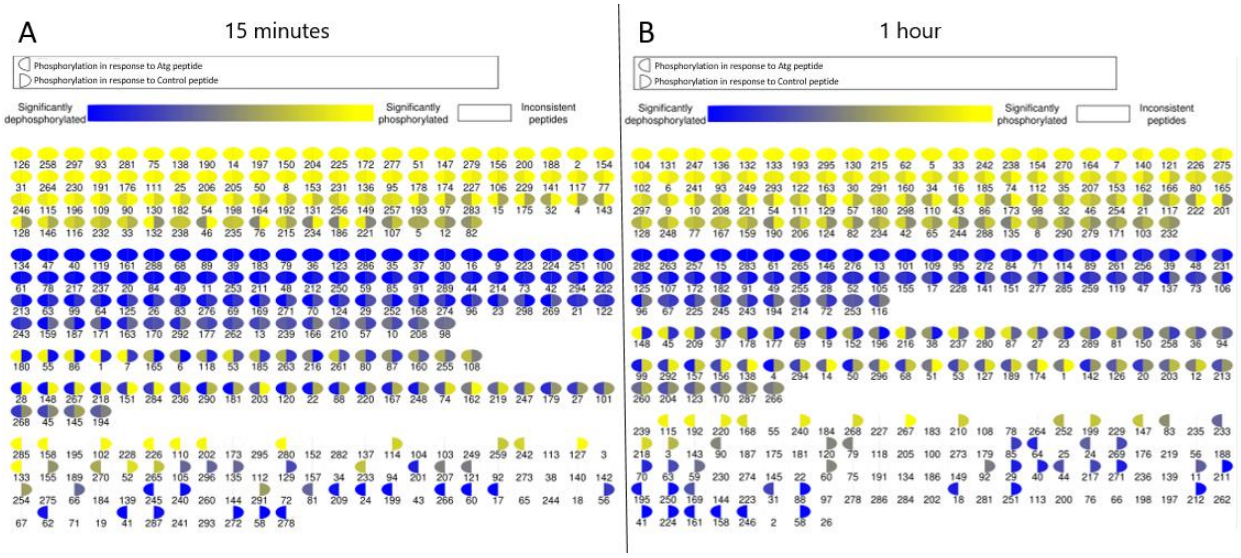

Figure 4-3. Differential phosphorylation of individual peptides revealed by kinome analysis. Results are given at 15 minutes (A) and 1 hour (B). Each spot represents a peptide. The left half represents phosphorylation in response to Atg peptide treatment, and the right half represents phosphorylation in response to Control peptide treatment. Yellow colouring indicates an increase in phosphorylation, compared to untreated samples, while blue colouring indicates a decrease in phosphorylation, compared to untreated samples. Blank spots indicate inconsistent spot identification by chi-squared testing.

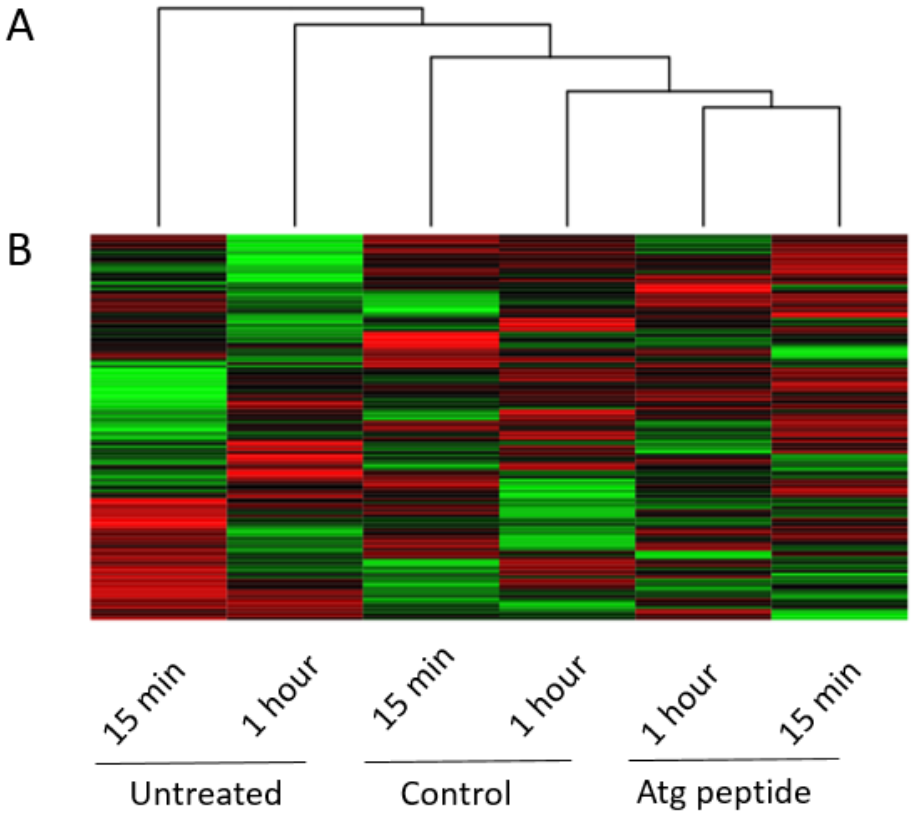

Figure 4-4. A dendrogram and heatmap of the hierarchical clustering of peptide phosphorylation status. Results are shown between untreated, Control and Atg peptide treated samples at 15 minutes and 1 hour.

($p<0.05$; FC>1.5 or FC<-1.5) between treatments (Atg peptide-treated and Control peptide-treated, both with Untreated signal background subtracted) are listed in Table 4-1. Several of the interesting results were selected for further analysis and validation of the approach (Table 4-2). From these results, several potential hypotheses regarding the mechanism of autophagy-inducing peptide cell death are discussed.

4.3 Objective 3: Validation of kinome array results by western blotting

Due to the nature and relative novelty of the kinome array technique and the associated results obtained, it was important to confirm our findings by Western blotting, a more conventional approach to analyzing protein phosphorylation cascades. The proteins described in Table 4-2 were evaluated in U937 cells stimulated with Atg peptide by Western blotting in an attempt to confirm kinome results.

4.3.1 p53 phosphorylation at S9 is induced by Atg peptide stimulation

U937 cells were stimulated with 30 μM Atg peptide for 15 min and 1 hr, similar to what was done for kinome analysis. Phosphorylation of p53 at residue S9 was found to be clearly upregulated in response to Atg peptide stimulation relative to untreated or control peptide-stimulated cells (Fig. 4-5). This observation was in line with findings of the kinome microarray experiments, which showed increased levels of S9 p53 phosphorylation at 15 minutes and 1 hour. Attempts were made to probe membranes with a total p53 antibody, but the signal was weak and inconsistent, and therefore not pursued further.

Table 4-1. Results from kinome analysis, detailing peptides whose phosphorylation was significantly altered in response to Atg peptide *vs* Control peptide treatments

Peptide	Time Point	FC
4E-BP1 S65	**15 mins**	**1.68014**
4E-BP1 S65	**1 hour**	**-1.62749**
4E-BP1 T70	1 hour	-1.51378
Akt1 S129	15 mins	1.59276
Akt1 S246	15 mins	-1.56296
Akt2 S474	1 hour	-2.28256
Akt3 S472	1 hour	-2.28908
AMPKA1 S496	1 hour	1.91664
AMPKA1 T183	1 hour	1.72595
AMPKB2 S108	15 mins	-2.75
AMPKB2 S182	1 hour	1.62512
ATG13 S361	1 hour	1.50592
ATG16L S269	15 mins	-1.77793
ATG9A S656	1 hour	1.71172
ATG9A S735	1 hour	2.04239
ATP1A1 Y10	**15 mins**	**-1.50138**
ATP1A1 Y10	**1 hour**	**1.59369**
Bad S134	1 hour	-1.69027
Bad S99	**15 mins**	**1.83465**
Bad S99	**1 hour**	**-1.81034**
Bax T167	15 mins	1.67298
beclin 1 S90	1 hour	1.7225
beclin 1 S93	1 hour	1.85351
beclin 1 Y352	15 mins	-2.50168
Casp3 S150	15 mins	1.75434

Peptide	Time Point	FC
Casp6 S257	1 hour	1.6673
Casp8 T448	15 mins	1.52859
Casp8 Y380	1 hour	1.53099
Casp9 S144	15 mins	1.55814
DAP S3	1 hour	-1.874
DAP3 S251	1 hour	-4.35563
DAP3 S280	15 mins	-1.80709
DAPK3 T306	15 mins	-1.68837
Deptor S265	15 mins	1.73139
Deptor S291	1 hour	1.91589
Drp1 S616	1 hour	-1.87181
Drp1 S637	1 hour	-1.76677
FOXO3A S232	1 hour	-1.71922
FOXO3A S294	1 hour	1.73568
FOXO3A S321	15 mins	-1.56201
FOXO3A S413	15 mins	-1.60947
FOXO3A S413	1 hour	1.82762
FOXO3A S588	1 hour	1.52675
FOXO3A T179	1 hour	-3.1739
IKKA S180	15 mins	-1.75676
IKKB Y199	15 mins	-2.13874
IKK-g S68	1 hour	-1.61915
JAK1 Y1035	1 hour	-1.80178
JAK2 Y570	1 hour	1.68788
JNK1 T183	15 mins	1.64446

Peptide	Time Point	FC
JNK1 T183	15 mins	1.64446
LST8 S43	15 mins	-2.22938
mTOR S1261	15 mins	-3.19607
mTOR S2448	1 hour	1.56013
mTOR T2474	1 hour	-1.6521
p53 S269	1 hour	1.77496
p53 S9	**15 mins**	**1.61027**
p53 S9	**1 hour**	**1.80894**
p53 T284	15 mins	2.35126
p53 T81	15 mins	-1.67525
RhoA S188	15 mins	-2.1987
rictor T1135	15 mins	-1.68878
SQSTM1 S332	1 hour	-2.22019
SQSTM1 S403	15 mins	1.58769
SQSTM1 T272	15 mins	1.7863
STAT3 S727	1 hour	1.58029
STAT3 Y705	15 mins	-2.2285
STAT6 Y641	15 mins	2.09547
TYK2 Y1054	1 hour	1.68486
ULK1 S638	15 mins	1.63341
UVRAG S689	1 hour	-2.04344
WDFY3 S2278	1 hour	-4.63466
WDFY3 S3339	1 hour	-2.38318

Significant difference in phosphorylation was defined as results with $p<0.05$, and a $FC>1.5$ or $FC<-1.5$. Bolded peptides were selected for further analysis and validation experiments.

Table 4-2. Differentially phosphorylated peptides chosen for further analysis

Protein	Phosphorylation	Functional implications
ATP1A1	Y10	This Na^+,K^+-ATPase was found to be required for autophagy-inducing peptide cell death. Y10 phosphorylation is associated with activation of pump. (Féraille et al., 1999)
4E-BP1	S65	S65 phosphorylation of 4E-BP1 has been associated with protection against rapamycin (an autophagy inducer) associated cell death. (Yellen et al., 2011)
Bad	S99	Part of the Bcl-2 superfamily of apoptotic regulators, S99 phosphorylation of Bad indicates exclusion from the mitochondria, preventing apoptosis. (Polzien et al., 2009)
p53	S9	A critical tumour suppressor protein, S9 phosphorylation likely plays a regulatory role in p53-mediated apoptosis. (Soubeyrand, Schild-Poulter, and Haché, 2004)

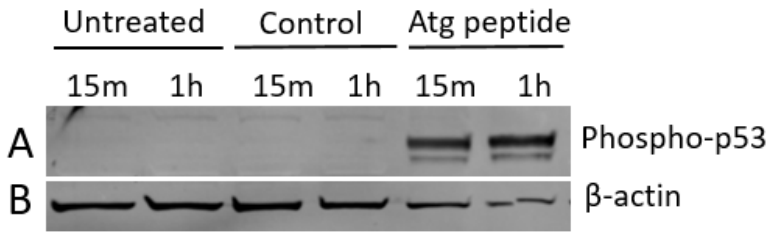

Figure 4-5. Western blot analysis of p53 protein phosphorylation at residue S9. U937 cells were treated with Atg peptide, Control peptide, or left untreated for 15 min and 1 hr. Bands of A) phospho-p53 were compared against B) β-actin expression. Antibodies directed against total p53 protein yielded a very weak and inconsistent signal that could not be used in further analysis (not shown.) Similar trends were observed in three separate experiments.

4.3.2 4E-BP1 phosphorylation at S65

Determining the phosphorylation status of 4E-BP1 was significantly more challenging than p53. There appeared to be little appreciable difference in the phosphorylated form of 4E-BP1 between treatments (Fig. 4-6A). Furthermore, the antibody directed against total 4E-BP1 revealed a few different species (Fig. 4-6B), making it difficult to distinguish the corresponding phosphorylated form detected using the phospho-4E-BP1-specific antibody. Of note also, β-actin expression was observed to be appreciably reduced in Atg peptide-treated cells (Fig. 4-6C). We attempted to use an alternative control protein, glyceraldehyde 3-phosphate dehydrogenase (GAPDH), but found similar results (not shown.) Therefore, Western blotting results need to be interpreted with caution. Indeed, when compared to β-actin expression, quantification of the bands detected for Phospho-4E-BP1 suggested an increase in S65 phosphorylation at both 15 minutes and 1 hour (Fig. 4-6D). However, when signal intensities were normalized against the total signal detected for the multiple species of 4E-BP1, the effect was reversed at 15 minutes or negligible at 1 hour between the Control and Atg peptide treatments (Fig. 4-6E). Kinome microarray results, on the other hand, suggested an increase in phosphorylation at 15 minutes but a decrease at 1 hour.

4.3.3 ATP1A1 phosphorylation at Y10

Y10-phosphorylation of ATP1A1 was also examined. Phosphorylated ATP1A1 appears to increase slightly in Atg-peptide treated samples, particularly at 1 hour post-stimulation (Fig. 4-7A). Interestingly, total ATP1A1 expression appears to increase concordantly (Fig. 4-7B). Similar quantification of the band intensities and comparison to β-actin levels indicated an increase in Y10-phosphorylation in response to Atg peptide stimulation (Fig. 4-7D). Normalization of the signals to total ATP1A1 expression showed a similar trend when comparing Atg peptide to Control

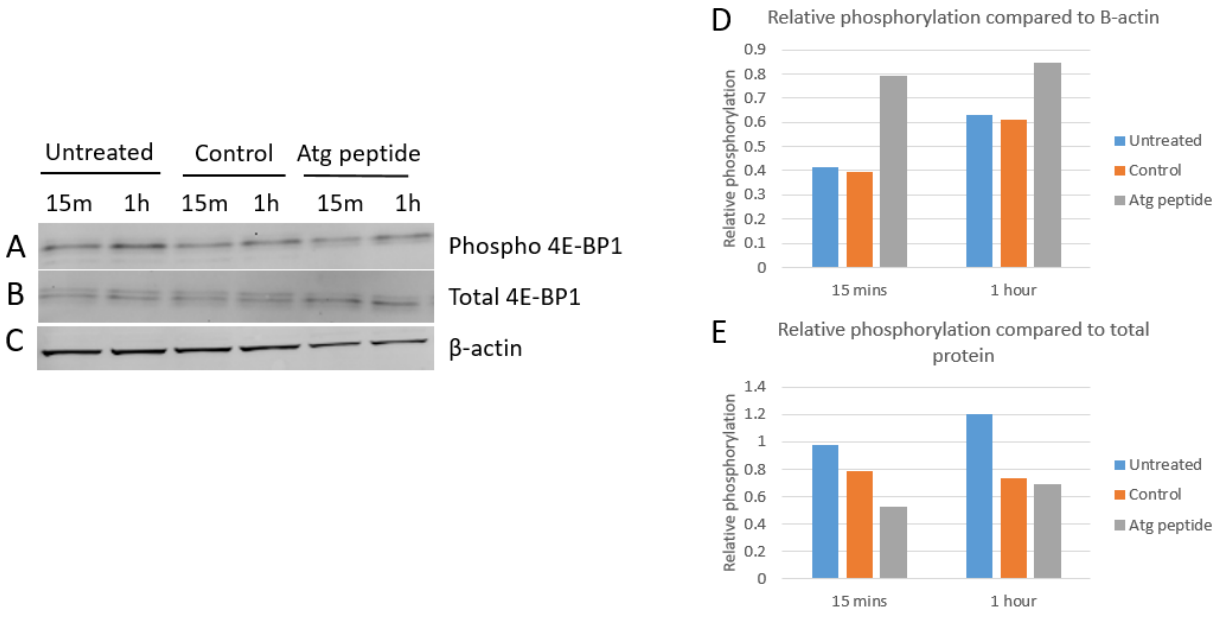

Figure 4-6. Western blot analysis of 4E-BP1 protein phosphorylation at residue S65. U937 cells were treated with Atg peptide, Control peptide, or left untreated for 15 min and 1 hr. Similar trends were observed with three different experiments.

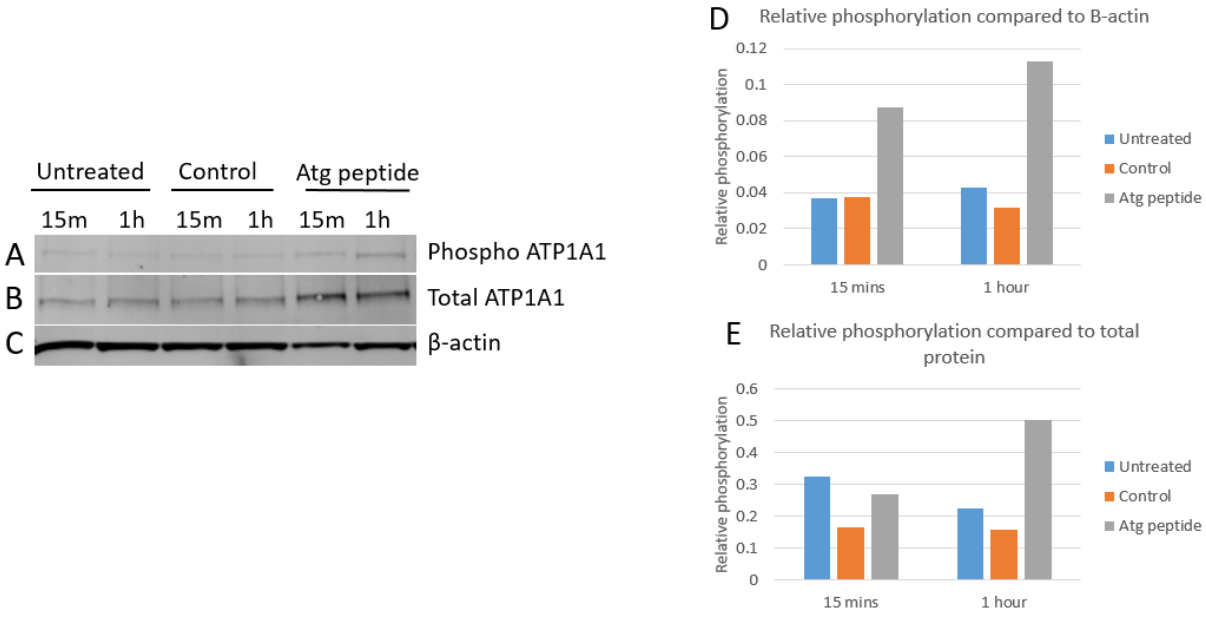

Figure 4-7. Western blot analysis of ATP1A1 protein phosphorylation at residue Y10. U937 cells were treated with Atg peptide, Control peptide, or left untreated for 15 min and 1 hr. Similar trends were observed in three separate experiments.

peptide (Fig. 4-7E). The kinome array results showed decreased levels of phosphorylation at 15 minutes, but increased levels at 1 hour, partially conforming to the Western blotting results.

4.3.4 Bcl-2 antagonist of cell death (Bad) phosphorylation at S99

Examination of the phosphorylation of the Bcl-2 antagonist of cell death (Bad) protein at S99 was attempted. However, the signal was extremely weak and not reliably quantifiable by Western blot, and thus it was not pursued further.

Chapter 5: Discussion

The importance of the autophagy pathway in cells is clear[3]. In addition to its role in regulating cellular homeostasis and mitigating cellular stress, we now know that autophagy plays an important role in cell death[22]. Our lab aims to elucidate the molecular mechanisms of monocytic cell death in response to cytokines such as IFNγ and IL-10, and more recently in response to an antimicrobial and autophagic cell death-inducing peptide[30].

5.1 U937 monocytic cells are an appropriate model for investigating cell death by kinome analysis

Using a flow cytometric approach, we examined U937 and primary human monocyte cell death in response to the Atg peptide. Both U937 and primary monocytes undergo Atg peptide-induced cell death, similar to what has been reported for other cell types[28]. This observation, along with the cell line's steady growth rates made it suitable for experiments that require large numbers of cells such as kinome analysis. However, given that it is an immortalized cell line with chromosomal abnormalities, it is quite possible that there would be significant differences in signalling response to the Atg peptide and other stimuli between U937 cells and primary monocytes. Therefore, if possible it would be ideal to pursue kinome analysis in primary human monocytes, which would be more physiologically relevant.

5.2 Kinome analysis identified multiple potential autophagic cell death signalling pathways

An autophagy and cell death pathway centric kinome array was successfully designed and tested in U937 monocytic cells to gain insight into the phosphorylation cascade that occurs as these

cells undergo autophagic cell death in response to the Atg peptide. This array will likely prove useful in similar investigations of other autophagic cell death stimuli and cell types in the future. Indeed, the kinome analysis revealed several potential pathways leading to autophagic cell death in monocytes, as discussed below.

5.2.1 The tumour suppressor protein p53 may be involved

The tumour suppressor protein p53 is involved in the cellular survival response, often in the case of repairing DNA damage. Several key regulatory phosphorylations on this protein were present on our array. Using kinome analysis, we visualized an increase in p53 S9 phosphorylation at both 15 minutes and 1 hour. Phosphorylation of p53 at S9 may have a role in p53-mediated apoptosis via activation of its transcriptional regulation properties[50]. p53 can also play both a positive or inhibitory role in the regulation of autophagy via both transcription-dependent and transcription-independent mechanisms[51]. Thus, I would hypothesize that S9 phosphorylation, as visualized by both kinome analysis and Western blotting, appears to play a positive role in Atg peptide-induced cell death, and presents an enticing target for further studies.

5.2.2 The transcription factor 4E-BP1 may be involved in autophagy-related cell death

4E-BP1 is a repressor of translation initiation that binds to the eIF4E factor and prevents its ability to initiate protein synthesis[52]. A previous study found that 4E-BP1 was capable of being phosphorylated at S65, and this phosphorylation was associated with protection against high-dose rapamycin-induced cell death[53]. Rapamycin is a potent inducer of autophagy, and thus the cell death occurring in this study may be similar to Atg peptide-induced cell death that we have seen.

Interestingly, we found that 4E-BP1 S65 phosphorylation was up-regulated at 15 minutes and down-regulated at 1 hour by kinome analysis. Since S65 phosphorylation confers protection against autophagy-related cell death, I hypothesized that this flux may indicate an initial resistance against cell death that is eventually downregulated and the cell succumbs. However, I was unable to confirm this phosphorylation trend by Western blot, and as such it would be prudent to further examine the role of 4E-BP1 in autophagic cell death using other methods.

5.2.3 An Na^+,K^+-ATPase involved in autophagic cell death was differentially phosphorylated

In a screen of potential inhibitors of autophagy-inducing peptide cell death, a class of compounds termed cardiac glycosides was found to be effective[28]. These molecules work to inhibit Na^+,K^+-ATPases, which suggests a role for these pumps in this novel form of autophagic cell death. A protein phosphorylation site on the α1 subunit of Na^+,K^+-ATPase was included in our array, and was found to be down-regulated early on at 15 minutes but up-regulated at 1 hour. Y10 phosphorylation has been associated with activation of the pump[54], and thus this novel result in monocytic cells lends support for a role of Na^+,K^+-ATPase pumps in this form of cell death. Na^+,K^+-ATPase has multiple functions within the cell that can all be potentially linked to the regulation of cell death[22]. The pump controls cellular resting potential, signal transduction, and cytoskeleton modifications such as attachment, motility and cell-cell interactions. Which of these functions contributes to autosis is yet to be elucidated, and it is likely that there are other important factors required in the signalling cascade as well. However, the Western blotting results show an increase in total ATP1A1 levels in response to stimulation with the Atg peptide, which may provide a mechanically distinct explanation for the increased level of phosphorylation at 1 hr by Western blot. Clearly, there is a need for more in-depth studies into this protein's role.

5.2.4 The potential involvement of the Bcl-2 family of autophagic and apoptotic regulators

The Bcl-2 family of proteins is involved in the regulation of both autophagy and apoptosis. Several proteins of the Bcl-2 family representing both positive and negative regulators of autophagy were present on our array. The Bad protein acts as an inhibitor of apoptosis and promotes autophagy via competitive disruption of the inhibitory interactions between Beclin 1 and one of the anti-apoptotic proteins of the Bcl-2 family[55]. Phosphorylation of S99 on the Bad protein was found to be up-regulated at 15 minutes and down-regulated by 1 hour. Phosphorylation of Bad at S99 has previously been shown to promote binding to 14-3-3 proteins, an association which down-regulates the apoptotic response and promotes cell survival[56]. I hypothesized that this phosphorylation may occur early in the response to stressors such as the Atg peptide, followed by dephosphorylation and an overwhelming cell death response. Similar to 4E-BP1, I was unable to confirm or refute this phosphorylation pattern due to an unreliably detectable signal by Western blotting, and thus there is a need for further analysis of Bad's role in autophagic cell death before any conclusions may be drawn.

5.2.5 Other notable kinome analysis results

There were notable phosphorylations, for example, on caspase 3 and caspase 8, both of which are involved in the proto-typical apoptotic cell death response. Caspase 3 phosphorylation at S150 was upregulated at 15 minutes, and caspase 8 phosphorylation at Y380 was upregulated at both 15 minutes and 1 hour. Interestingly, both of these phosphorylation events have been associated with inhibition of their respective activation, thus potentially inhibiting apoptotic mechanisms[57]. Additionally, caspase 6 phosphorylation at S257 was upregulated at 1 hour, and

phosphorylation of this residue leads to caspase 6 inhibition and suppression of apoptotic cell death[58]. This lends further support to the caspase-independent nature of autophagic cell death which occurs in response to the Atg peptide[22].

Another interesting phosphorylation event that was found by kinome analysis in response to the Atg peptide is the phosphorylation of p62 on residue S403. This phosphorylation was found to be upregulated at 15 minutes, and is associated with an increased affinity of this protein for polyubiquitinated proteins and stabilization of its cargo for autophagosome entry[59]. This may implicate a form of heightened and/or selective, chaperone-mediated autophagy in autosis, and presents an interesting area for further studies.

5.3 Kinome analysis is subject to some limitations

While kinome analysis is a powerful tool for the examination of molecular responses, and while every effort is made to reduce errors, it is also subject to some limitations. For example, we now know that the molecular environment of kinase-substrate phosphorylation reactions can be a key regulatory measure. Environmental solubility, pH, and physical access to substrate peptides are all important aspects to facilitate phosphorylations, as well as other signalling mechanisms. For example, Taelman et al. found that Wnt signaling causes sequestration of Glycogen Synthase Kinase 3 from the cytosol into multivesicular bodies, separating the kinase from its cytosolic substrates[60]. In another example, phosphorylation of Akt within the activation T-loop causes a charge-induced change in conformation that facilitates further substrate binding[61]. It can be difficult, or nearly impossible, to emulate these conditions in the lab, especially as part of an *in silico*, high-throughput experiment such as kinome analysis. Individual peptides on a solid support

can be quite different from *in vivo* cellular conditions. Thus, we must recognize that this data represents a starting point, and certainly further analysis of these phenomena is needed.

Kinome analysis also provides a means for high-throughput experimentation, the results of which can then be finely examined and further probed more directly and concretely. We attempted to confirm the kinome results using Western blotting techniques, with somewhat mixed results (Table 5-1). p53 phosphorylation at S9 appears to be induced by the Atg peptide, similarly to what was found by kinome analysis, whereas Y10 phosphorylation of ATP1A1 and S65 phosphorylation of 4E-BP1 results are not entirely concordant. Given the difference in targets for the two assays, namely the *capacity* of cellular lysates to phosphorylate targets in kinome analysis versus the *quantity* of phosphorylated proteins detected by Western blotting, it is not entirely surprising that there were some inconsistencies. The discrepancies observed emphasize the need for further confirmatory approaches, such as genetic alteration of impugned signalling pathways or silencing RNAs, which would more directly implicate the given cellular signalling pathway or molecule.

Table 5-1. A comparison of kinome and Western blotting results

Protein (Phosphorylation)	Time Point	Kinome Result	Western Result
p53 (S9)	15 mins	Increased	Increased
	1 hr	Increased	Increased
4E-BP1 (S65)	15 mins	Increased	Unclear
	1 hr	Decreased	Unclear
ATP1A1 (Y10)	15 mins	Decreased	Unclear
	1 hr	Increased	Increased

Chapter 6: Conclusion

High-throughput experimentation methods are becoming more and more prominent in many scientific domains. The importance of post-translational protein modifications as cell signaling events positions the kinome microarray as an important instrument for rapidly screening the intricate molecular mechanisms of many cellular functions.

An *in vitro* model to study the regulation of programmed cell death in monocytic cells using an autophagic cell-death-inducing peptide was successfully developed. Both primary human monocytes and cells of the U937 monocytic line reacted similarly to stimulation with Atg peptide. I subsequently designed and tested an autophagy-centric kinome microarray, which also contained many other cell death-related peptides. Several peptides correlating to proteins of interest were found to be differentially phosphorylated between Atg peptide and Control peptide treatments using kinome analysis. These included a member of the Bcl-2 cell death family, the p53 tumour suppressor protein, and a Na^+,K^+-ATPase transporter protein, the latter having been found to be required for Atg peptide-induced death[28]. Western blotting with phospho-specific antibodies was conducted to confirm kinome array results. Although there was a clear concordance when comparing kinome and Western blot results in the case of p53 for example, there were discrepancies, as noted above and in Table 5-1. These discrepancies may be explained in part by the differing natures of these two assays as well as their differing methods of analysis. Namely, kinome microarrays evaluate the capacity of cellular lysates containing kinases and phosphatases to modulate the phosphorylation of proteins/peptides of interest, whereas Western blots detect the phosphorylation status of these respective protein targets.

Nevertheless, our autophagy-centric kinome array is a valuable screening tool for cell death signalling events. It will serve as a guide for subsequent functional studies aimed at more directly

delineating the molecular mechanisms responsible for autophagic cell death in monocytic cells in this case, and will surely be applied to other model systems.

Chapter 7: References

1. Klionsky, D. J. Autophagy revisited: A conversation with Christian de Duve. *Autophagy* **4,** 740–743 (2014).

2. Klionsky, D. J. *et al.* Guidelines for the use and interpretation of assays for monitoring autophagy. *Autophagy* **8,** 445–544 (2012).

3. Deretic, V., Saitoh, T. & Akira, S. Autophagy in infection, inflammation and immunity. *Nat. Rev. Immunol.* **13,** 722–737 (2013).

4. Huang, W. & Klionsky, D. J. Autophagy in Yeast : A Review of the Molecular Machinery Autophagy and related vacuolar trafficking pathways. **420,** 409–420 (2002).

5. Thompson, A. R. & Vierstra, R. D. Autophagic recycling: lessons from yeast help define the process in plants. *Curr. Opin. Plant Biol.* **8,** 165–73 (2005).

6. Bassham, D. C. *et al.* Autophagy in Development and Stress Responses of Plants. *Autophagy* **2,** 2–11 (2014).

7. Ravikumar, B. *et al.* Regulation of mammalian autophagy in physiology and pathophysiology. *Physiol. Rev.* **90,** 1383–435 (2010).

8. Noda, T., Suzuki, K. & Ohsumi, Y. Yeast autophagosomes : de novo formation of a membrane structure. **12,** 231–235 (2002).

9. Longatti, A. & Tooze, S. A. Vesicular trafficking and autophagosome formation. *Cell Death Differ.* **16,** 956–65 (2009).

10. Jaber, N. & Zong, W. X. Class III PI3K Vps34: Essential roles in autophagy, endocytosis, and heart and liver function. *Ann. N. Y. Acad. Sci.* **1280,** 48–51 (2013).

11. Kroemer, G., Mariño, G. & Levine, B. Autophagy and the integrated stress response. *Mol. Cell* **40,** 280–93 (2010).

12. Geeraert, C. *et al.* Starvation-induced hyperacetylation of tubulin is required for the stimulation of autophagy by nutrient deprivation. *J. Biol. Chem.* **285,** 24184–94 (2010).

13. Mortimore, G. E. & Pösö, A. R. Intracellular protein catabolism and its control during nutrient deprivation and supply. *Annu. Rev. Nutr.* **7,** 539–64 (1987).

14. Brady, N. R., Hamacher-Brady, A., Yuan, H. & Gottlieb, R. a. The autophagic response to nutrient deprivation in the hl-1 cardiac myocyte is modulated by Bcl-2 and sarco/endoplasmic reticulum calcium stores. *FEBS J.* **274,** 3184–97 (2007).

15. Webb, J. L., Ravikumar, B., Atkins, J., Skepper, J. N. & Rubinsztein, D. C. Alpha-Synuclein is degraded by both autophagy and the proteasome. *J. Biol. Chem.* **278,** 25009–13 (2003).

16. Kim, I., Rodriguez-Enriquez, S. & Lemasters, J. J. Selective degradation of mitochondria by mitophagy. *Arch. Biochem. Biophys.* **462,** 245–53 (2007).

17. Coussens, L. M. & Werb, Z. Inflammation and cancer. *Nature* **420,** 860–867 (2002).

18. Biet, F., Locht, C. & Kremer, L. Immunoregulatory functions of interleukin 18 and its role in defense against bacterial pathogens. *J. Mol. Med.* **80,** 147–162 (2002).

19. Dinarello, C. A. Immunological and inflammatory functions of the interleukin-1 family. *Annu. Rev. Immunol.* **27,** 519–50 (2009).

20. Guermonprez, P., Valladeau, J., Zitvogel, L., Théry, C. & Amigorena, S. Antigen Presentation and T Cell Stimulation by Dendritic Cells. *Annu. Rev. Immunol.* **20,** 621–667 (2002).

21. Eisenberg-Lerner, A., Bialik, S., Simon, H.-U. & Kimchi, A. Life and death partners: apoptosis, autophagy and the cross-talk between them. *Cell Death Differ.* **16,** 966–75 (2009).

22. Liu, Y. & Levine, B. Autosis and autophagic cell death: the dark side of autophagy. *Cell Death Differ.* 1–10 (2014). doi:10.1038/cdd.2014.143

23. Fimia, G. M. & Piacentini, M. Toward the understanding of autophagy regulation and its interplay with cell death pathways. *Cell Death Differ.* **16,** 933–4 (2009).

24. Elmore, S. Apoptosis: a review of programmed cell death. *Toxicol. Pathol.* **35,** 495–516 (2007).

25. Fink, S. & Cookson, B. Apoptosis, pyroptosis, and necrosis: mechanistic description of dead and dying eukaryotic cells. *Infect. Immun.* **73,** (2005).

26. Ouyang, L. *et al.* Programmed cell death pathways in cancer: a review of apoptosis, autophagy and programmed necrosis. *Cell Prolif.* **45,** 487–98 (2012).

27. Maiuri, M. C. *et al.* Control of autophagy by oncogenes and tumor suppressor genes. *Cell Death Differ.* **16,** 87–93 (2009).

28. Liu, Y. *et al.* Autosis is a Na+,K+-ATPase-regulated form of cell death triggered by autophagy-inducing peptides, starvation, and hypoxia-ischemia. *Proc. Natl. Acad. Sci. U. S. A.* **110,** 20364–71 (2013).

29. Sridhar, S., Botbol, Y., Macian, F. & Cuervo, A. M. Autophagy and disease: always two sides to a problem. *J. Pathol.* **226,** 255–73 (2012).

30. Shoji-Kawata, S. *et al.* Identification of a candidate therapeutic autophagy-inducing peptide. *Nature* **494,** 201–6 (2013).

31. Kumar, H., Kawai, T. & Akira, S. Pathogen recognition by the innate immune system. *Int. Rev. Immunol.* **30,** 16–34 (2011).

32. Serbina, N. V, Jia, T., Hohl, T. M. & Pamer, E. G. Monocyte-Mediated Defense Against Microbial Pathogens. *Annu. Rev. Immunol.* **26,** 421–452 (2008).

33. Aderem, A. & Underhill, D. M. Mechanisms of phagocytosis in macrophages. *Annu. Rev. Immunol.* **17,** 593–623 (1999).

34. English, L. *et al.* Autophagy enhances the presentation of endogenous viral antigens on MHC class I molecules during HSV-1 infection. *Nat. Immunol.* **10,** 480–7 (2009).

35. Italiani, P. & Boraschi, D. From monocytes to M1/M2 macrophages: Phenotypical vs. functional differentiation. *Front. Immunol.* **5,** 1–22 (2014).

36. Martinez, F. O. & Gordon, S. The M1 and M2 paradigm of macrophage activation: time for reassessment. *F1000Prime Rep.* **6,** 13 (2014).

37. Orvedahl, A. & Levine, B. Eating the enemy within: autophagy in infectious diseases. *Cell Death Differ.* **16,** 57–69 (2009).

38. Liu, Q. *et al.* Autophagy sustains the replication of porcine reproductive and respiratory virus in host cells. *Virology* **429,** 136–47 (2012).

39. Shi, Y. Serine/Threonine Phosphatases: Mechanism through Structure. *Cell* **139,** 468–484 (2009).

40. Diks, S. H. *et al.* Kinome profiling for studying lipopolysaccharide signal transduction in human peripheral blood mononuclear cells. *J. Biol. Chem.* **279,** 49206–13 (2004).

41. Hornbeck, P. V. *et al.* PhosphoSitePlus, 2014: Mutations, PTMs and recalibrations. *Nucleic Acids Res.* **43,** D512–D520 (2015).

42. Jalal, S. *et al.* Genome to kinome: species-specific peptide arrays for kinome analysis. *Sci. Signal.* **2,** pl1 (2009).

43. Arsenault, R. J. *et al.* Kinome analysis of Toll-like receptor signaling in bovine monocytes. *J. Recept. Signal Transduct. Res.* **29,** 299–311 (2009).

44. Trost, B., Arsenault, R., Griebel, P., Napper, S. & Kusalik, A. DAPPLE: a pipeline for the homology-based prediction of phosphorylation sites. *Bioinformatics* **29,** 1693–5 (2013).

45. Li, Y. *et al.* A systematic approach for analysis of peptide array kinome data. *Sci. Signal.* **5,** pl2 (2012).

46. Alhetheel, A. *et al.* Amplification of the signal transducer and activator of transcription I signaling pathway and its association with apoptosis in monocytes from HIV-infected patients. *AIDS* **22,** 1137–44 (2008).

47. Alhetheel, A. HIV-induced dysregulation of IFN-gamma signaling and programmed cell death in primary human monocytes. (Doctoral dissertation). (2010).

48. Belmokhtar, C. A., Hillion, J. & Ségal-Bendirdjian, E. Staurosporine induces apoptosis through both caspase-dependent and caspase-independent mechanisms. *Oncogene* **20,** 3354–3362 (2001).

49. Bradford, M. M. A rapid and sensitive method for the quantitation of microgram quantities of protein utilizing the principle of protein-dye binding. *Anal. Biochem.* **72,** 248–54 (1976).

50. Soubeyrand, S., Schild-Poulter, C. & Haché, R. J. G. Structured DNA promotes phosphorylation of p53 by DNA-dependent protein kinase at serine 9 and threonine 18. *Eur. J. Biochem.* **271,** 3776–3784 (2004).

51. Levine, B. & Abrams, J. p53: The Janus of autophagy? *Nat. Cell Biol.* **10,** 637–9 (2008).

52. Yanagiya, A. *et al.* Translational Homeostasis via the mRNA Cap-Binding Protein, eIF4E. *Mol. Cell* **46,** 847–858 (2012).

53. Yellen, P. *et al.* High-dose rapamycin induces apoptosis in human cancer cells by dissociating mTOR complex 1 and suppressing phosphorylation of 4E-BP1. *Cell Cycle* **10,** 3948–3956 (2011).

54. Féraille, E. *et al.* Insulin-induced stimulation of Na+,K(+)-ATPase activity in kidney proximal tubule cells depends on phosphorylation of the alpha-subunit at Tyr-10. *Mol. Biol. Cell* **10,** 2847–59 (1999).

55. Mariño, G., Niso-Santano, M., Baehrecke, E. H. & Kroemer, G. Self-consumption: the interplay of autophagy and apoptosis. *Nat. Rev. Mol. Cell Biol.* (2014). doi:10.1038/nrm3735

56. Polzien, L. *et al.* Identification of novel in vivo phosphorylation sites of the human proapoptotic protein BAD. Pore-forming activity of bad is regulated by phosphorylation. *J. Biol. Chem.* **284,** 28004–28020 (2009).

57. Alvarado-Kristensson, M. *et al.* p38-MAPK signals survival by phosphorylation of caspase-8 and caspase-3 in human neutrophils. *J. Exp. Med.* **199,** 449–58 (2004).

58. Velázquez-Delgado, E. M. & Hardy, J. A. Phosphorylation Regulates Assembly of the Caspase-6 Substrate-Binding Groove. *Structure* **20,** 742–751 (2012).

59. Matsumoto, G., Wada, K., Okuno, M., Kurosawa, M. & Nukina, N. Serine 403 phosphorylation of p62/SQSTM1 regulates selective autophagic clearance of ubiquitinated proteins. *Mol. Cell* **44,** 279–289 (2011).

60. Taelman, V. F. *et al.* Wnt signaling requires sequestration of Glycogen Synthase Kinase 3 inside multivesicular endosomes. *Cell* **143,** 1136–1148 (2010).

61. Scheid, M. P. & Woodgett, J. R. Unravelling the activation mechanisms of protein kinase B/Akt. *FEBS Lett.* **546,** 108–112 (2003).